ISTANBUL TECHNICAL UNIVERSITY ★ GRADUATE SCHOOL OF SCIENCE ENGINEERING AND TECHNOLOGY

EFFECT OF NOZZLE EXIT GEOMETRY ON THE JET FLOW

M.Sc. THESIS

Yavuzer KARAKUŞ

Department of Aeronautics and Astronautics Engineering

Aeronautics and Astronautics Engineering Program

Supervisor: Assist. Prof. Dr. Duygu ERDEM

JANUARY 2015

ISTANBUL TECHNICAL UNIVERSITY ★ GRADUATE SCHOOL OF SCIENCE ENGINEERING AND TECHNOLOGY

EFFECT OF NOZZLE EXIT GEOMETRY ON THE JET FLOW

M.Sc. THESIS

Yavuzer KARAKUŞ

511111170

Department of Aeronautics and Astronautics Engineering

Aeronautics and Astronautics Engineering Program

Supervisor: Assist. Prof. Dr. Duygu ERDEM

JANUARY 2015

Yavuzer Karakus, a M.Sc. student of ITU Institute of Science and Technology student ID 511111170, successfully defended the thesis/dissertation entitled "EFFECT OF NOZZLE EXIT GEOMETRY ON THE JET FLOW", which he prepared after fulfilling the requirements specified in the associated legislations, before the jury whose signatures are below.

Thesis Advisor : **Assist. Prof.Dr. Duygu ERDEM** ....

Istanbul Technical University

Jury Members : **Assist. Prof.Dr. Duygu ERDEM** ....

Istanbul Technical University

Assist. Prof.Dr. K. Bülent YUCEIL ....

Istanbul Technical University

Assist. Prof.Dr. Murat CAKAN ....

Istanbul Technical University

Date of Submission : 15 December 2014

Date of Defense : 20 January 2015

FOREWORD

I would like to thank my advisor Duygu Erdem for all the help and support she has provided. Also would like to thank my mother, Zeynep Karakus, for the care she gave during the times I worked hard.

JANUARY 2015 Yavuzer KARAKUŞ

TABLE OF CONTENTS

Page

ABBREVIATIONS

2D	: Two Dimensional
3D	: 3 Dimensional
BSA	: Burst Spectrum Analyzer
CAD	**:** Computer Aided Design
CFD	**:** Computational Fluid Dynamics
CNC	**:** Computer Numerical Control
DNS	**:** Direct Numerical Simulation
HAD	**:** Hesaplamalı Akışkanlar Dinamiği
k-ε	**:** k-epsilon
LDA	**:** Laser Doppler Anemometry
LES	**:** Large Eddy Simulation
M	**:** Mach Number
PC	: Personal Computer
PRESTO	**:** Pressure Staggering Option
RANS	**:** Reynolds Averaged Navier Stokes
Re	**:** Reynolds Number
S-A	**:** Spallart Allmaras
TKE	**:** Turbulence Kinetic Energy

LIST OF TABLES

Page

LIST OF FIGURES

Page

LIST OF SYMBOLS

$\mathbf{d}$	**:** Nozzle Exit Diameter
$\mathbf{u}$	**:** Velocity in the jet direction, i.e. x axis
$\mathbf{u'}$	**:** Velocity fluctuation in the jet direction, i.e. x axis
$\mathbf{u_{rms}}$	**:** Root mean square of velocity fluctuations on x axis
$\mathbf{U}$	**:** Flow velocity
$\mathbf{U_0}$	**:** Maximum velocity in the domain
$\mathbf{U_c}$	**:** Velocity on the centerline at the x position
$\mathbf{v}$	**:** Velocity in the y direction
$\mathbf{v'}$	**:** Velocity fluctuation in the y direction
$\mathbf{v_{rms}}$	**:** Root mean square of velocity fluctuations on y axis
$\mathbf{w}$	**:** Velocity in the z direction
$\mathbf{w'}$	**:** Velocity fluctuation in the z direction
$\mathbf{w_{rms}}$	**:** Root mean square of velocity fluctuations on z axis

EFFECT OF NOZZLE EXIT GEOMETRY ON THE JET FLOW

SUMMARY

Nozzles have a widespread usage in the industrial and daily life. For example, combustion chambers, air conditioning systems, jet engine exhausts are nozzles from which high speed jet flow issues. There are problems with the jet flow as well, such as noise which is a source of noise pollution and mixing problems which results in performance reduction. Solution to these problems is disguised in the flow phenomena. That is why understanding the jet flow and parameters affecting it is an important subject. Through this study, effect of the exit geometry of a nozzle on the flow issuing from it was investigated. Firstly nozzles were designed in the light of past work. Different geometrical aspects were tried to be included in the work. CAD drawings were generated. CFD analyses were conducted on the predetermined nozzle geometries after generating a mesh structure on the measurement volume. Secondly, flow parameters were experimentally measured with the help of an LDA system. LDA system settings were adjusted to have an optimum data rate. Necessary post-processing was conducted and results were compared with the CFD data to validate the CFD methodology. A valid CFD methodology was constructed to be used in further research.

JET AKIŞINDA LÜLE ÇIKIŞ GEOMETRİSİNİN ETKİSİ

ÖZET

Jet akışı bir yapı tarafından yönlendirilerek bir başka akışkan ortamının içine hızla akan akış olarak tanımlanabilir. Bu hedef akış da belirli bir hıza sahip olabileceği gibi durağan bir ortam, örneğin atmosfer, de olabilir. Jet akışı endüstriyel ve günlük uygulamalarda yaygın olarak kullanılması sebebiyle mühendislik açısından ayrıca önem arz etmektedir. Kullanım alanları olarak yanma odaları, havalandırma sistemleri, karıştırıcılar, jet motorlarının egzoz akışları vs. verilebilir. Burada jet akışlarından kaynaklı sorunlardan da söz edilebilir. Bunlara örnek olarak uçak motorlarının egzoz gürültüsü, havalandırma sistemlerinde oluşan gürültüler, yakıt-hava karışımında yaşanan sıkıntılardan bahsedilebilir. Bunların çözümü jet akışının yapısını anlamaktan geçmektedir. Hangi parametrelerin hangi akış özellikleri ve yapılarını etkilediğini anladığımız takdirde sorunları çözmek için yöntemler geliştirebiliriz. Bu açıdan jet akışı üzerine etkisi olan etmenler mühendislik açısından çekici bir konu haline gelmektedir.

Bu çalışmada bir lüleden çıkan jet akışı ele alınacaktır. Lüle çıkış geometrisinin önemi yüksektir. Bu konu üzerinde bazı çalışmalar yapılmış ve lüle çıkış geometrisinin jet akışı üzerinde etkili bir parametre olduğu ortaya çıkmıştır. Bazı çalışmalarda yonca şeklinde, yaprak sayısına göre isim almaktadır, lüleler ile çalışılmış ve olumlu sonuçlar alınmıştır. Ancak bu etkilerin kısa süreli olduğu görülmüştür. Bir diğer şekil ise dörtgen şeklinde olanlardır. Burada köşeli çıkış geometrilerinin köşe etkisi sebebiyle yuvarlak lülelere göre daha etkin olduğu görülmüştür. Burada etkinden kasıt hem gürültü hem de karışımı açısından önemli olan karıştırma hızının yüksek olmasıdır. Karıştırma hızı jet akışı ile dış akış arasındaki hız farkının ne kadar hızlı azaldığının da bir ölçüsüdür ve yüksek olması tercih edilmektedir.

Çalışmada 3 tane çıkış geometrisi ele alınacaklardır, bunlar yuvarlak, 3 yapraklı yonca ve eşkenar dörtgen geometrileridir. Bu çıkış geometrilerine sahip lüleler çıkış alanları aynı olacak şekilde yapılandırılacaklardır. Aynı zamanda giriş alanları da eşit olacaktır. Böylece tek etkenin çıkış geometrisi olduğu varsayımı yapılacaktır. Lülelerin hepsi simetrik olduğu için bu özellik de çalışmada zaman kazandırıcı yönde kullanılmıştır

Öncelikli olarak belirlenen lüle konseptleri incelendikten sonra ölçülendirmeler yapılmıştır. Bu ölçülendirmeler test sisteminin yapısı, gerekli hata payı limitlerinin sağlanması, detaylı ölçüm alınabilecek kadar büyük ama sistem hava akışı kapasitesini aşmayacak kadar küçük ölçüler kullanılması hedef alınarak gerçekleştirilmiştir.

Ölçüler belirlendikten sonra Bilgisayarlı Mühendislik programlarıyla katı model halinde hazırlanmıştır. Daha sonra gerekli akış alanı ölçümlendirmeleri yapılıp akış alanlarının CAD modelleri hazırlanmıştır. Bu akış alanları için ticari bir Hesaplamalı Akışkanlar Dinamiği, HAD, programına entegre mesh programı vasıtasıyla ağ yapısı hazırlanmıştır. Çalışmanın sayısal kısmında bazı geometriler için simetri ve bazı geometriler için periyodiklik kabulü yapılmıştır. Böylece bilgisayar kaynağı gereksinimi azaltılmıştır. Bu ağ yapısı ile gerekli sınır ve başlangıç şartları da kullanılarak HAD analizleri gerçekleştirilmiştir. 3 geometri için HAD çalışmaları gerçekleştirilmiştir.

Bu geometrilerden 2si aynı zamanda deneysel çalışmada kullanılmıştır. Yuvarlak lüle alüminyum malzemeden CNC tezgâhında üretilmiştir. Eşkenar dörtgen lüle ise 3 boyutlu yazıcı ile üretilmiştir. Bu lülelerin dinlenme odasına bağlanması için gerekli parçada çalışma esnasında tasarlanıp pleksiglas malzemeden CNC tezgahda üretilmiştir. Deneysel çalışmalarda Laser Doppler Anemometry, LDA, yöntemi kullanılarak hız alanı ölçümleri gerçekleştirilmiştir. Buradan ortalama ve türbülanslı akış parametreleri hesaplanmıştır. LDA sisteminin ayarları yapılarak, gerekli parametrelerin en uygun seviyelere gelmesi sağlanmıştır.

Sayısal ve deneysel çalışma sonuçları karşılaştırılarak sayısal çözüm gerçeklenmiştir. Aynı zamanda çıkış geometrisi ve akış üzerine etkisi ile ilgili değerlendirmeler yapılmıştır. Bu aşamadan sonra CFD sonuçları karşılaştırılarak lüle çıkış geometrisinin akış üzerine etkisi sayısal olarak belirlenmeye çalışılmıştır. Gerekli iyileştirme ve gelecek dönemde konu üzerine yapılmasının yararlı olacağı düşünülen çalışmalar değerlendirilmiştir.

1. INTRODUCTION

Fluid ejected from a nozzle into a resting or flowing medium produced a free jet flow (Gohil et al., 2014). Relationship between jet geometries and their flow field characteristics is significant in many engineering fields. Efficiency of many applications of jet flow, such as ejectors, propulsive systems and HVAC systems, is heavily connected to the mixing features of the jet flow (Yukselenturk and Erdem, 2012). Enhanced mixing is requested in jet propulsion applications to lower plume temperature and infrared radiation levels while controlling flow unsteadiness reduces aerodynamic noise in jet engines (Hilgers, 2000) Performance of these devices can be enhanced by understanding the characteristics of jet flow at higher Re (Gohil et al., 2014).

The geometry of the nozzle is a primary parameter at this point. Circular nozzles are axisymmetric and widely used, but a great interest is present on different nozzles and their effects on the characteristics of the flow. Non circular jets gained much interest primarily due to their potential of enhanced mixing between jet flow and surroundings (Gutmark and Grinstein, 1999). Lobed nozzles or other modified nozzle shapes have been reported to provide faster spreading and some research reported noise reduction as well (Zaman, Wang and Georgiadis, 2002). Strong axial vorticity, which is effective in mixing supersonic flows, is induced by lobed nozzles which also provide the same thrust level as the axisymmetric nozzles (Gutmark and Grinstein, 1999). However, effect of the lobed nozzle is limited to some extent (two diameters), the mixing structure after this limit is the same as that of circular jet (Hu et al.). Nozzles with sharp corners are the other non circular nozzle type of interest. There are different properties of these nozzles contributing to the flow. Mass entrainment and fine scale turbulence is increased significantly at the corners in comparison to the flat segments by the introduction of sharp corners in the nozzle (Schadowet et al, 1988),(Toyoda and Hussein, 1989) and (Vandsburger and Ding, 1995). As a consequence, different nozzle exit geometries are of interest of both academic and industrial research. An example of an aircraft exhaust nozzle with a noncircular exit profile is shown in Figure 1.1.

Figure 1.1 : Noncircular aircraft exhaust nozzle.

Numerical tools such as CFD codes are important to visualize and study the fluid flow without experimental set-up, saving time and funds. Application of the appropriate numerical scheme in the computations is a key factor of CFD analysis. Also validation of the numerical results to check the convenience of the domain, mesh, boundary conditions and numerical scheme is required to rely on the analysis.

In this study a commercial CFD code has been used to investigate the flow field of jet flow from different nozzle geometries. Firstly present experimental results were used to validate the numerical method used and then various nozzle geometries were used to see their effects on the jet flow.

2. METHOD

2.1. Nozzles

In the conceptual design phase three nozzle exit geometries were determined to be used in the study. They were circular, 3 lobed and rhombus geometries. The reason for these geometries was to see the effect of both lobes and corners on the jet flow as they are interesting geometries in the jet flow studies. The sketches of these geometries are shown in Figure 2.1.

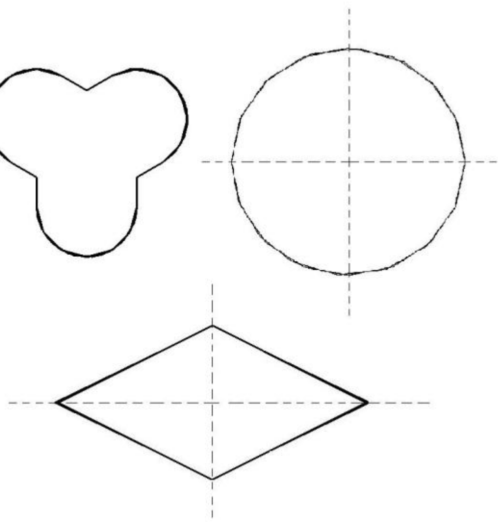

Figure 2.1 : Sketches of the nozzle exit geometries.

After the selection of the nozzle exit geometries appropriate nozzle dimensions were determined. A good contraction profile was the main concern while dimensioning the nozzle. An inlet diameter of 60mm and an exit diameter of 20mm were selected with a nozzle length of 75mm to avoid flow separation. Nozzle exit diameter were determined both to be able to maintain high subsonic velocity range and minimize percentage errors in the experimental processes.

CAD drawings were prepared in CATIA. Nozzles were designed to be easily mounted/demounted to the settling chamber. A connector part was designed to mount the nozzles to the settling room, which also directs the flow to the nozzle and reduces the material and labor costs while manufacturing the nozzle. CAD drawings of the nozzles are shown in Figure 2.2.

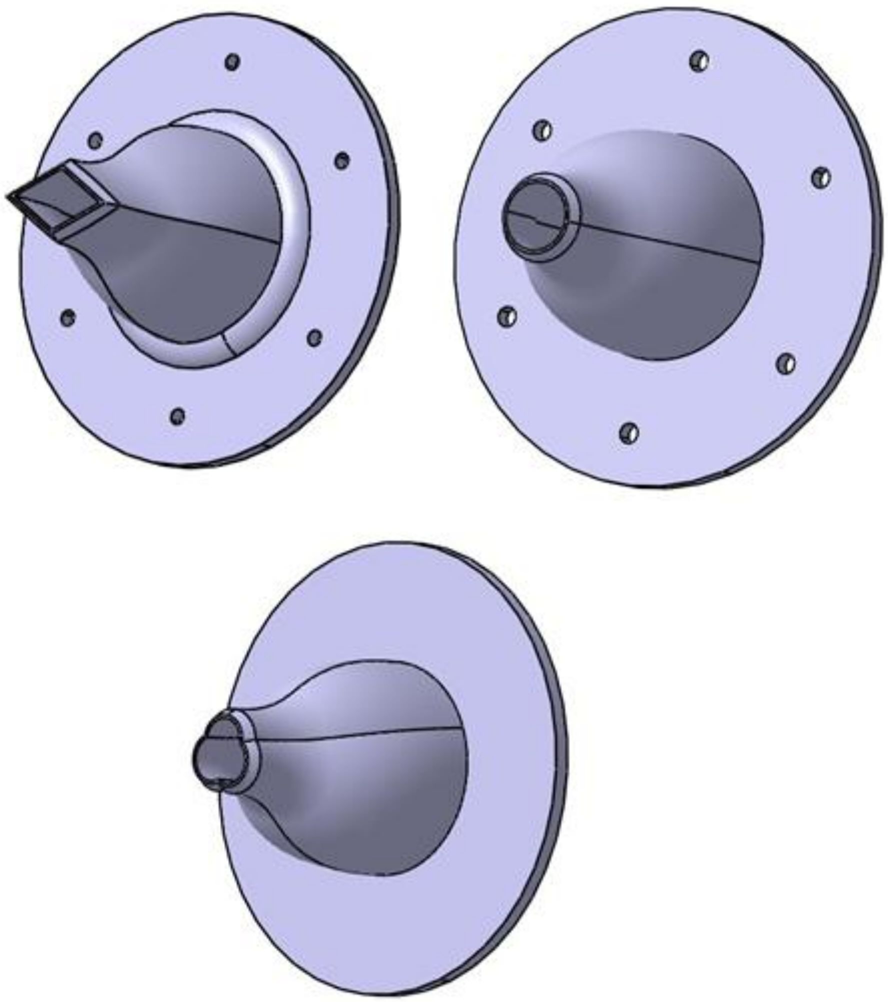

Figure 2.2 : CAD drawings of the nozzles used in the study.

Nozzles were manufactured by means of different techniques. Circular nozzle was manufactured in the CNC workshop of Trisonic Lab, while rhombus geometry was manufactured by 3D printing. Sharp corners of the rhombus geometry cannot be manufactured by CNC machining as a radius would be needed in the corners, thus it was decided to use 3D printing instead. Rhombus nozzle which is ready to use is shown in Figure 2.3.

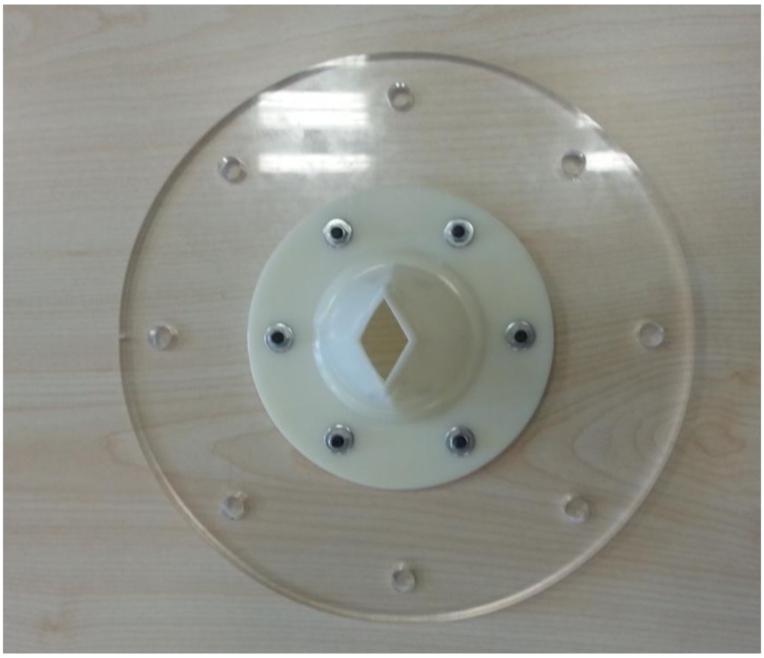

Figure 2.3 : 3D printed Rhombus type nozzle connected to the connector part.

CFD domain was also generated in CATIA, to let it be easy to use in mesher software. Importing geometry would be easier then drawing it from scratch in mesh software as their CAD capabilities are limited. How the domain geometries and dimensions were decided is stated in the CFD section. After determining the dimensions and shape of the CFD domains, the nozzles and their connector part is removed from the bulk shape of the domain to leave the fluid domain only. Examples of the CFD domain are shown in the CFD section.

For the velocity range Mach number of 0.8 was determined to work in the high subsonic region. Compressibility effects are not negligible so compressible jet flow would be the area of interest. Required settling chamber pressure was calculated using the compressible flow relations.

2.2. CFD

CFD analyses were conducted using a commercial solver. Mesh was generated in ICEM CFD software. After mesh was generated it was imported into the CFD software, FLUENT, and boundary conditions, material properties, turbulence model, discritization schemes and under relaxation factors were selected. Plots were constructed to visualize the convergence in critical or pre-determined regions of the flow or on the boundaries.

CFD domains of various nozzles were degraded into smaller part by the help of the nozzle being symmetric, axi-symmetric or periodic. For the rhombus and circular nozzle domain symmetry was taken into account and ¼ of the domain in the radial direction was taken as the domain to be used in the CFD analysis. In the 3 lobed case as the geometry consists of three equal lobes, a 120^0 slice was taken and periodic boundaries were used. As an example, the domain used for the 3 lobed case is shown in Figure 2.4.

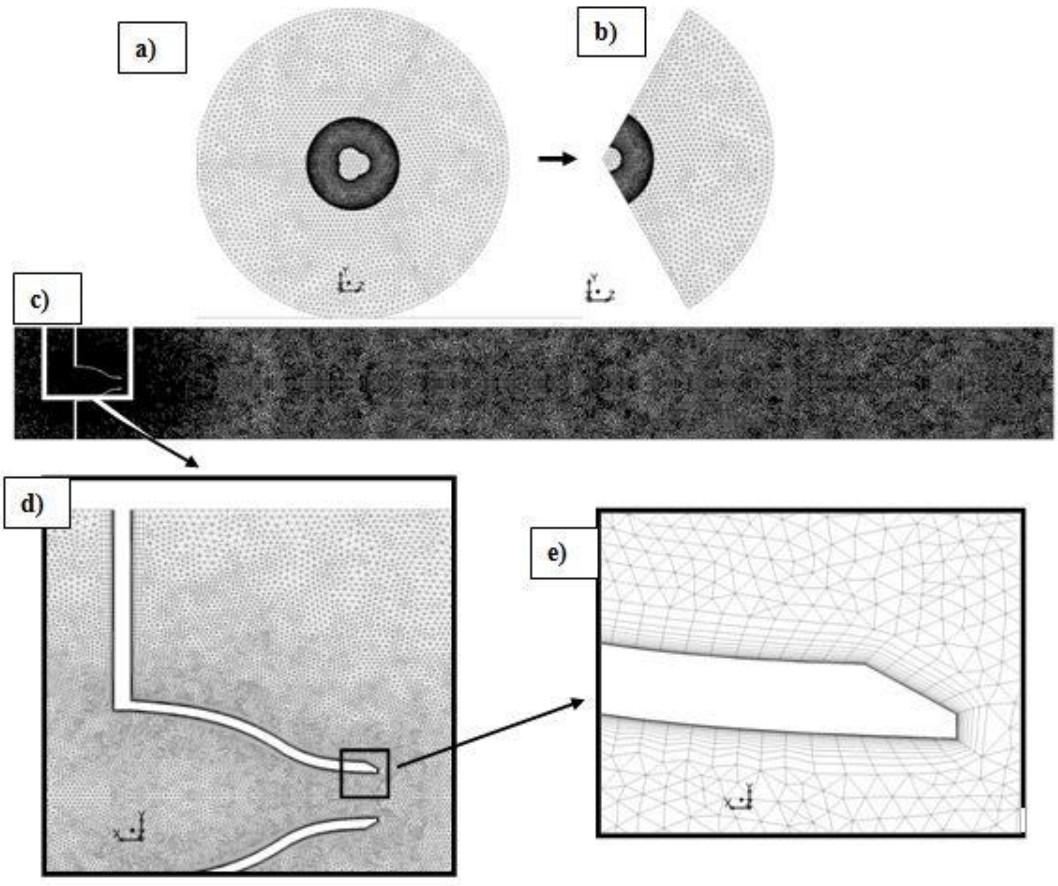

Figure 2.4 : An overview of the mesh structure for 3 lobed geometry. a) is the view from the inlet b) is the view from the inlet of the real CFD domain (slice of 120 degree) c) is the cross-sectional view of the CFD domain (periodic surface are seen) d) close up view of the nozzle section e) boundary layer mesh.

An overview of the mesh is shown in Table 2.1 to show the general properties of the mesh system.

Table 2.1 : An overview of the mesh.

Geometry	Number of cells	Mesh type
Circular	~3M	Tetrahedrons with boundary mesh in near wall regions
Rhombus	~3M	Tetrahedrons with boundary mesh in near wall regions
3 lobed	4M	Tetrahedrons with boundary mesh in near wall regions

Pressure based solver was used as it is compatible with both low and high speed flows contrary to its past and lowers the computational costs. Reynold Averaged Navier Stokes turbulence models were decided to be used because they require less computer resources and give the required flow data for his study. RANS models models the whole flow in contrast to LES where only small eddies are modeled while large eddies are solved directly and DNS where all of the domain is solved numerically. Thus LES and DNS requires much more computer resources as they demand mesh sizes small enough to contain the eddies they try to solve.

An appropriate RANS model was discussed to be used in numerical computations. k-ε viscous model provided strong agreement with experimental data for nearfield jet entrainment (Garcia, 2007)., so k-ε models were concentrated on. CFD code which was used has offered standard, renormalization group (RNG) and realizable k-ε models, of which RNG and realizable are modified versions of the standard model. As stated in the theory guide of the CFD code, realizable k-ε model is relatively recent development of the three models and has a new formulation for the turbulent viscosity and a new transport equation for the dissipation rate (ε). Consistency with the physics of the turbulent flows is achieved by satisfying mathematical constraints on Reynolds stresses. An immediate benefit of the realizable k-ε model is that it more accurately predicts the spreading rate of both planar and round jets (ANSYS Inc., 2009). That's why realizable k-ε RANS model with enhanced wall treatment was used, as it is a more accurate version of the k-ε model.

SIMPLE method was used for the pressure-velocity coupling. Discritization schemes were Green Gauss node based for gradient, PRESTO for pressure. PRESTO scheme was used because this procedure has mainly the same computational approach with the staggered-grid schemes which are run on structured meshes and results have nearly the same accuracy for triangular, tetrahedral, hybrid and polyhedral meshes (Fluent Inc., 2006). Density, momentum, turbulence kinetic energy, turbulent dissipation rate and energy were discretized with second order upwind scheme.

2.3. Experimental

Laser Doppler Anemometry was used to measure the velocity field thus turbulence parameters. Jet flow rig of the Trisonic Research Lab. was used in the experimental work. Experimental setup consists of Dantec Instruments BSA LDA system placed on a ISEL traverse System. LDA system & traverse system is controlled together with BSA flow software. Flow to the settling room is controlled by a regulator with ER3000 valve. The rig consists of a high pressure air source controlled by the pneumatic regulator to sustain a constant settling chamber pressure. The regulator is controlled by a computer system to which a pressure transducer is connected via an A/D card. The software of the regulator is used to control the regulator and a Labview code runs to feedback the required analog signal for the pressure to the regulator. Settling room is a tube to which the pressure transducer to feedback pressure to the regulator control system and seeder is connected. Seeder is a Laskin nozzle system which produces olive oil particles to seed the system for LDA visibility. A general view of the Jet Flow rig is shown in Figure 2.5 and Figure 2.6

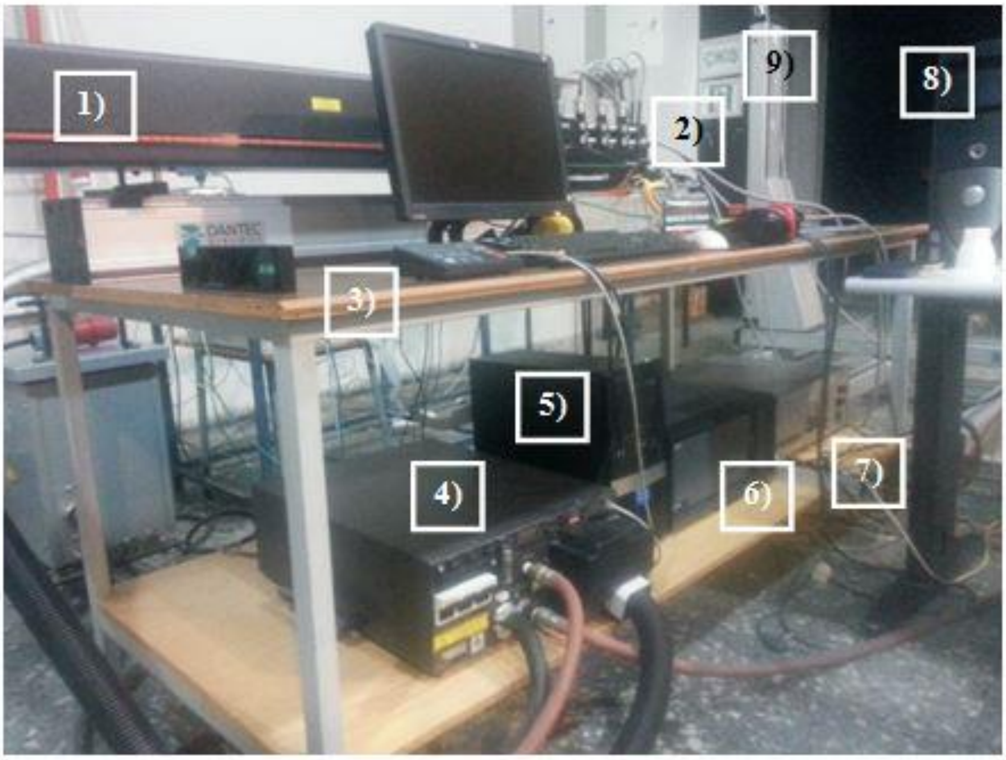

1) Laser head
2) Transmitter
3) Laser system controller
4) Laser producer
5) Pressure regulator controller PC
6) BSA (Burst Spectrum Analyzer)
7) Traverse controller
8) LDA PC
9) Traverse system

Figure 2.5 : Jet flow set-up at Trisonic Research Lab -1.

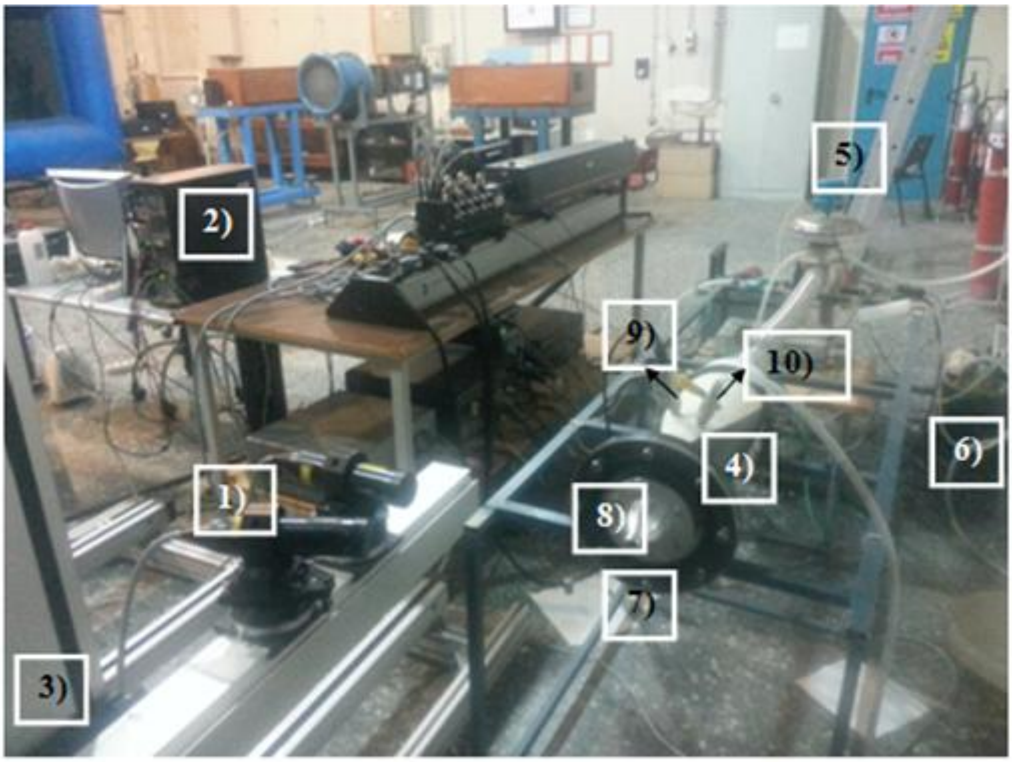

1) LDA probes
2) LDA PC
3) Traverse system
4) Settling room
5) ER 3000 regulator
6) Laskin nozzle
7) Pleksiglas connector
8) Nozzle
9) Pressure transducer
10) Seeding inlet

Figure 2.6 : Jet flow set-up at Trisonic Research Lab -2.

Firstly, settings of the LDA system were done. Laser source settings were done on the two main parts of the system, laser head and transmitter. On the laser head two knobs are present to set the mirror angles to direct the laser light to the inlet of the transmitter. When directed properly by the help of the PEAK function of the controller, the power output of the laser head is maximized. Then the setting knobs, which are six for each laser beam, on the transmitter were used to focus the light to the fiber optic cables to ensure the power and shape of the beams. This was done by eye control while the laser source ran at low power setting. Pin hole setting was done previously so no move was done to change this setting.

After finishing the laser beam power settings, burst settings in the BSA Flow software were set. Burst settings consists of center frequency, bandwidth, record length, record length mode, high voltage level, signal gain, burst detector SNR level. These settings are important to have a good burst signal thus healthy data. Each parameter had different values for each setting station. Setting stations were determined by the change in data rate, validation and burst signal. When condition of the signal went worse, the settings were replenished for that part of the domain. Setting stations were determined at x/d ratios of 5, 15 and 30. At these stations burst signal, validation and data rate were optimized by intuition.

After the settings were determined for the domain, a fast scan was done to determine the domain limits in the y direction. Limits were important both to have shorter data collection times and not to lose any data by choosing a narrow domain. At the pre-described stations a fast scan with 5mm intervals were accomplished in the y direction. Limits for the domains in the y direction were determined

After the domain limits were set, x axis which is the jet centerline and y axis which is the axis perpendicular to the jet centerline were scanned. X axis was scanned up to 40d while y axis scans were made at x/d ratios of 0.3, 2, 5, 10, 15, and 20 with a limit on y which was determined previously by the fast scan conducted.

3. RESULTS AND DISCUSSION

To compare the flow structures of the three jet flows velocity distribution and turbulence intensity were the parameters selected to visualize the flow. Experimental data was taken in 2D. Due to this fact, parameters in the validation section were calculated in 2D. CFD data has been in 3D, so transformation from 3D to 2D was done.

Firstly CFD validation was conducted to evaluate the accuracy of the CFD results. Distribution of dimensionless x velocity on the jet centerline (x axis) is shown in Figure 3.1. Nearly x/d=10 is the location where velocity values differ between experimental and CFD results. Difference makes a peak around x/d=20, but then decreases.

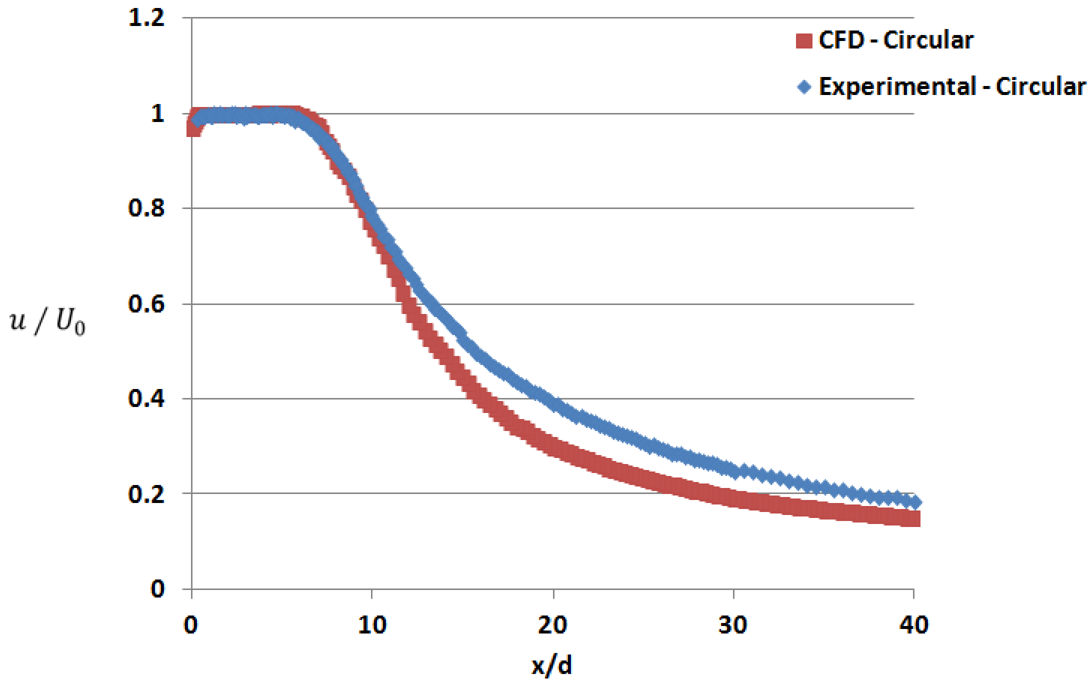

Figure 3.1 : u/U_0 vs x/d for circular nozzle validation case.

Turbulence intensity distribution on the jet centerline for circular exit profile is shown in Figure 3.2. Starting with a difference at the jet exit, the difference diminishes while approaching x/d=10. This is interpreted to be due to the complexity of the flow at that region which the turbulence model could not solve accurately due to its limitations on turbulence modeling.

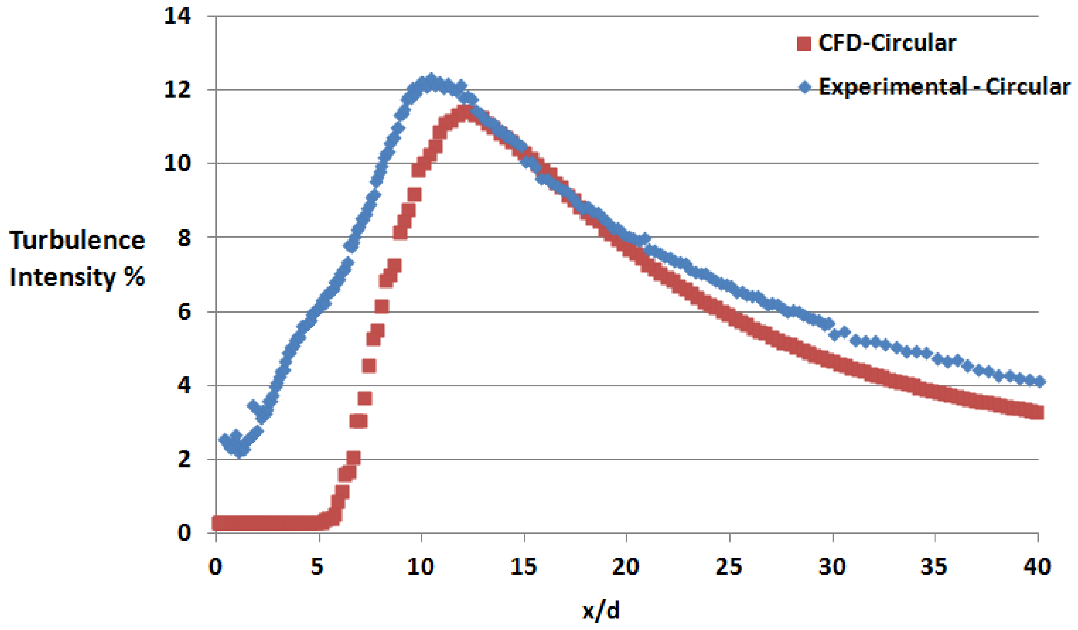

Figure 3.2 : Turbulence intensity distribution on the jet centerline for circular nozzle validation case.

In Figure 3.3 dimensionless u velocity, v velocity and turbulence intensity distribution on a plane perpendicular to the jet axis at x/d=0.3 is shown. In this case experimental and CFD data are in good agreement. A small shift in the experimental data is seen and that was interpreted to be due to orientation and numerical errors.

In Figure 3.4 dimensionless u velocity, v velocity and turbulence intensity distribution on a plane perpendicular to the jet axis at x/d=2 is shown. A small shift in the experimental data was seen and that was interpreted to be due to orientation and numerical errors. v velocity distribution inside the jet shows difference, but the difference diminishes approaching to jet borders. The reason behind this is the inability of the realizable k-ε model to predict the radial velocity accurately.

Figure 3.5 and Figure 3.6 show dimensionless u velocity, v velocity and turbulence intensity distribution in the direction perpendicular to the flow at x/d=5 and x/d=10 respectively. The difference between the turbulence intensity at x/d=10 increased when compared with previous regions. But the difference between v velocity values of CFD and experimental data decreases when moved in the downstream direction, i.e. x direction.

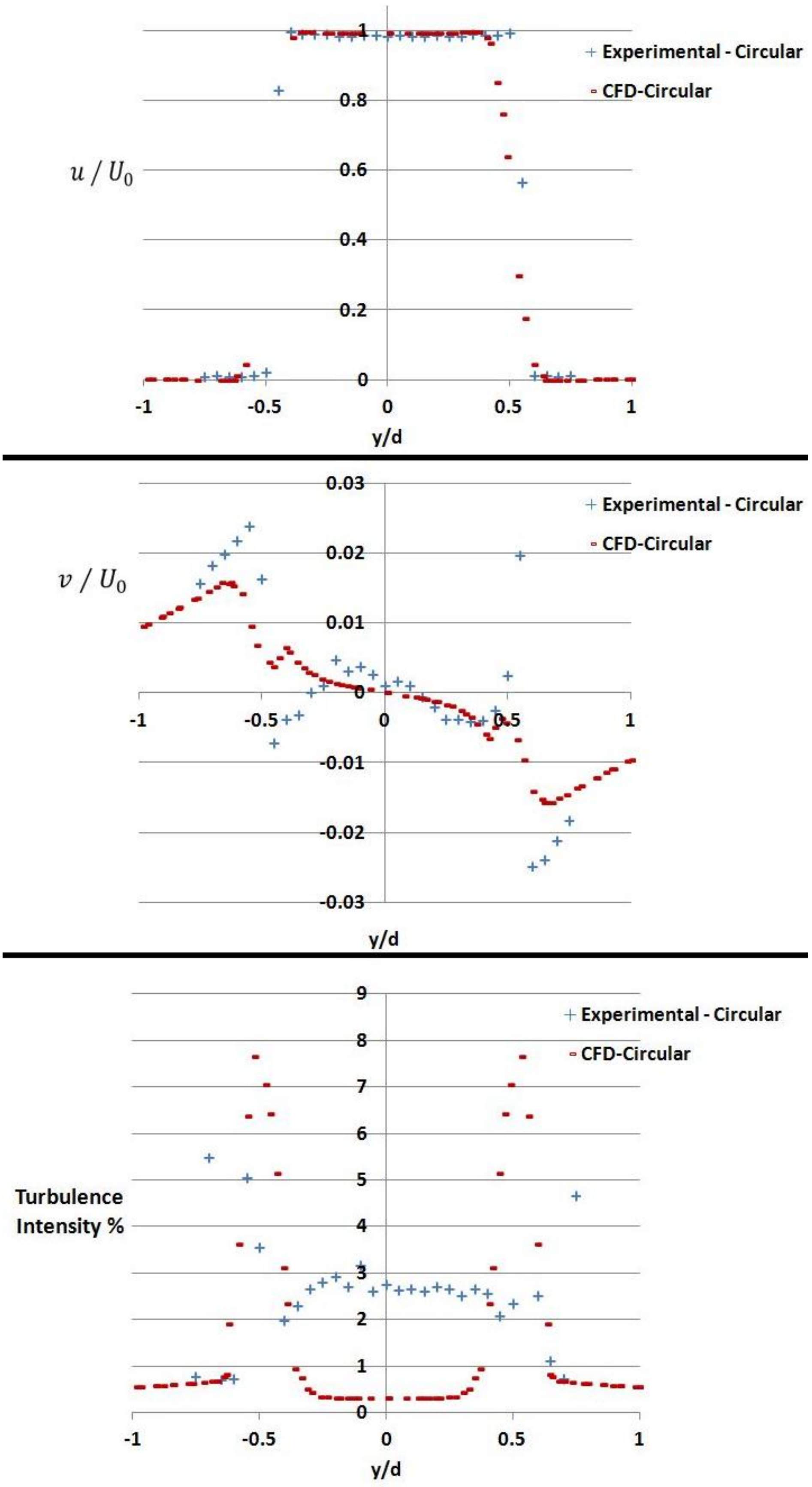

Figure 3.3 : Dimensionless u velocity, v velocity and turbulence intensity distribution in the direction perpendicular to the flow at x/d=0.3.

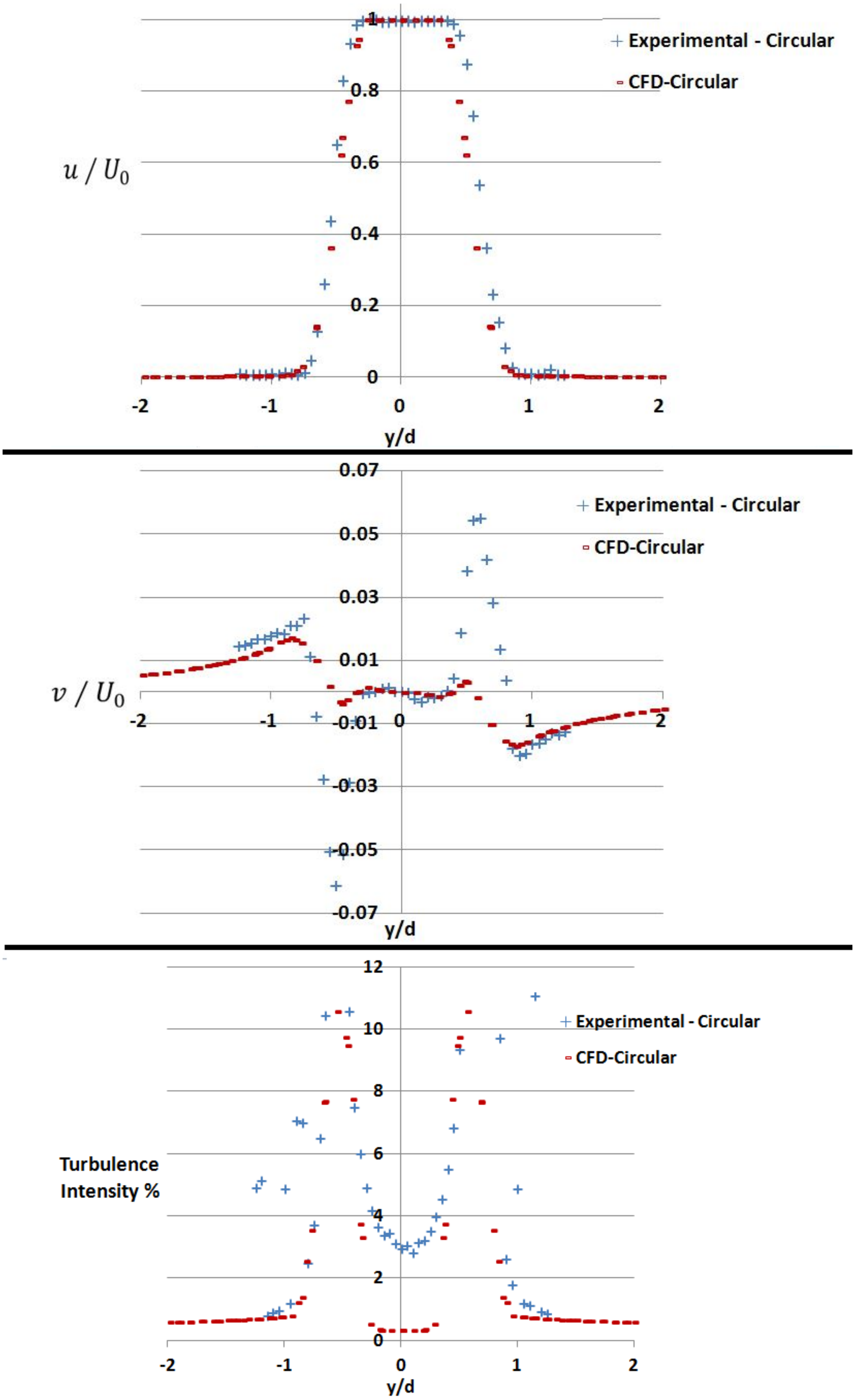

Figure 3.4 : Dimensionless u velocity, v velocity and turbulence intensity distribution in the direction perpendicular to the flow at x/d=2.

Distribution of the flow parameters at the plane x/d=20 is shown in Figure 3.7. The difference which was shown in the jet centerline distributions can be seen. u velocity of the CFD decayed faster than the experimental results, while v velocity continues to converge to the experimental counterpart. The difference of turbulence intensity is the same as x/d=10.

In general CFD results show good agreement with the experimental results. In some regions deviations from experimental data is present but the trends are always parallel to the experimental data. It is acceptable to use the CFD method mentioned in this section for comparison of jet flows issuing from different nozzle exit geometries. However, using the CFD results directly in real world needs extra care for certain regions and parameters.

The assumption of isotropic turbulence in k-ε turbulence model made it difficult to compare Reynolds stress components separately. Thus u_{rms}, v_{rms} and $\overline{u' x\, v'}$ parameters were depicted as experimental results at x/d=0.3, 2, 5, 10 and 20 yz planes. u_{rms}, v_{rms} and $\overline{u' x\, v'}$ distributions are shown in Figure 3.8, Figure 3.9 and Figure 3.10 respectively.

u_{rms} levels are low near the nozzle exit. At x/d=2 and 5 a maximum level is reached with a value of 0.18. Then it decreases downstream. But the profile get smoother while moving downstream. This can be seen explicitly at x/d=2 and 5 as their maximum is the same but the profile is smoother at x/d=5. At x/d=20 two peaks nearly emerged into one signaling the start of the self-similar region.

v_{rms} profiles has the same trend as u_{rms} However, the maximum values are lower when compared with u_{rms} at the same x/d plane. The profiles get smoother faster than u_{rms}, so the distribution at x/d=20 has only one peak.

$\overline{u' x\, v'}$ distribution has two extremum points each x/d position. The distance between the extremum points increases while moving downstream, however, the amplitude decreases. Up to x/d=5 the effect of the potential core can be seen in the center region with a value of 0.

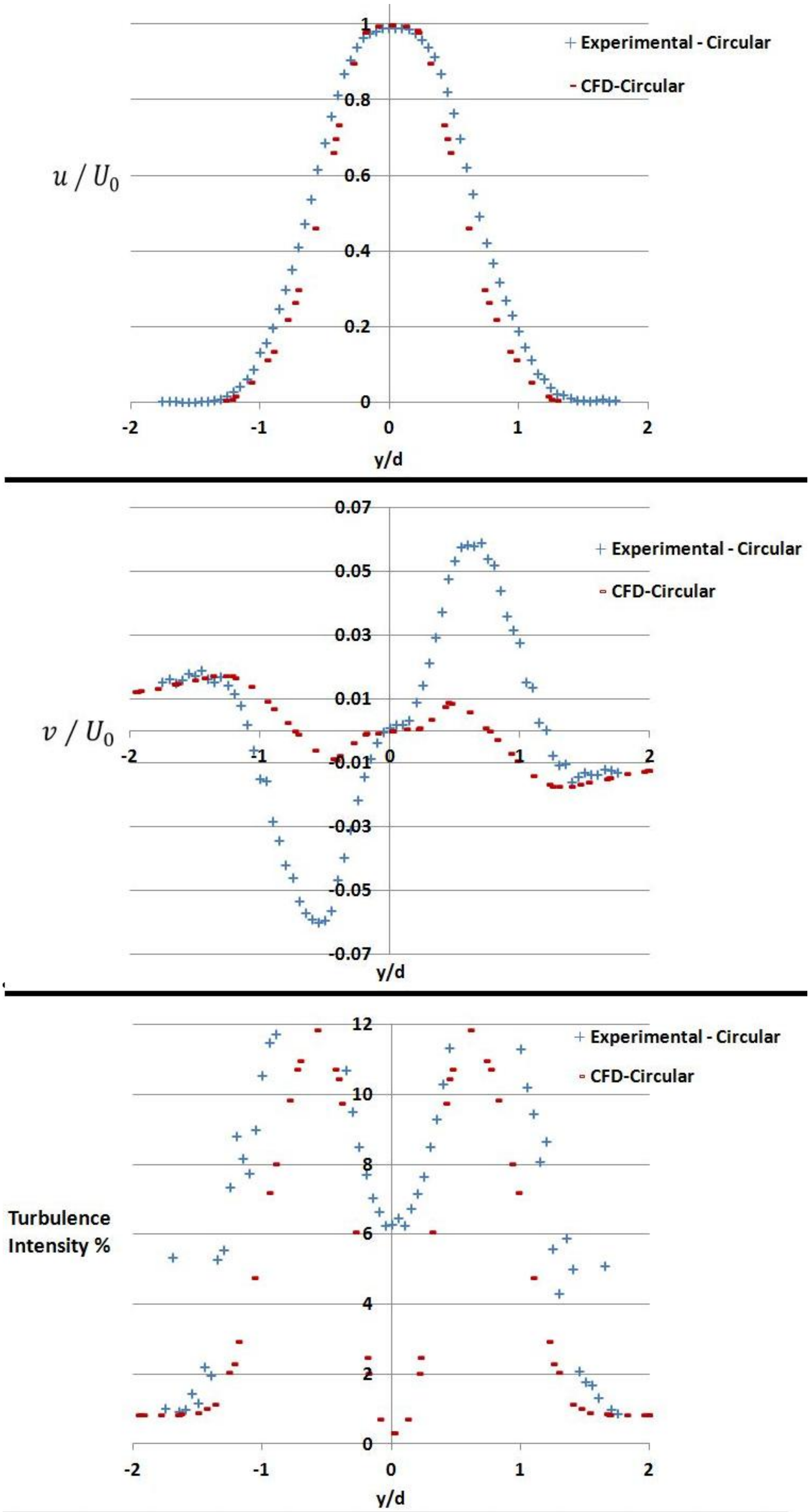

Figure 3.5 : Dimensionless u velocity, v velocity and turbulence intensity distribution in the direction perpendicular to the flow at x/d=5.

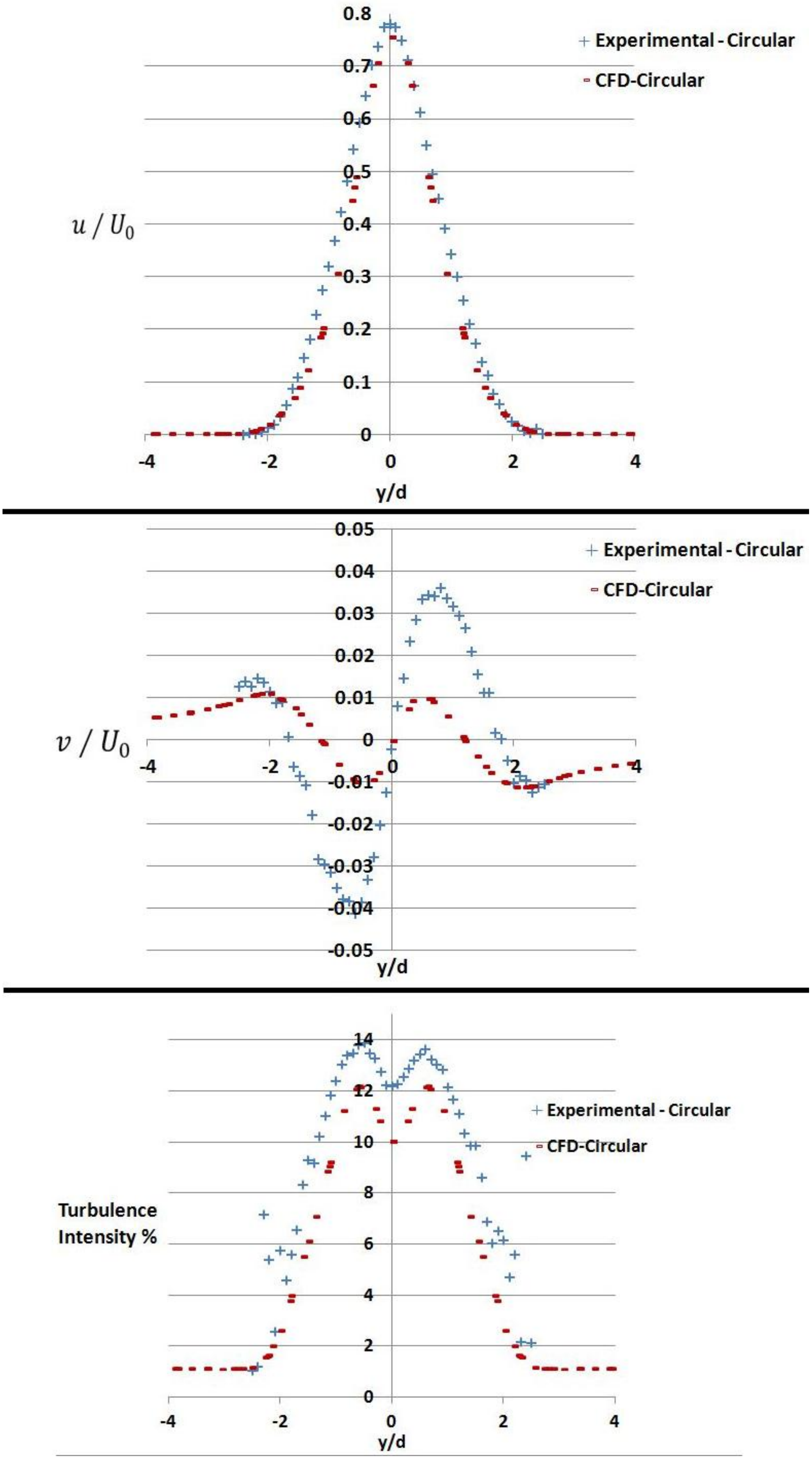

Figure 3.6 : Dimensionless u velocity, v velocity and turbulence intensity distribution in the direction perpendicular to the flow at x/d=10.

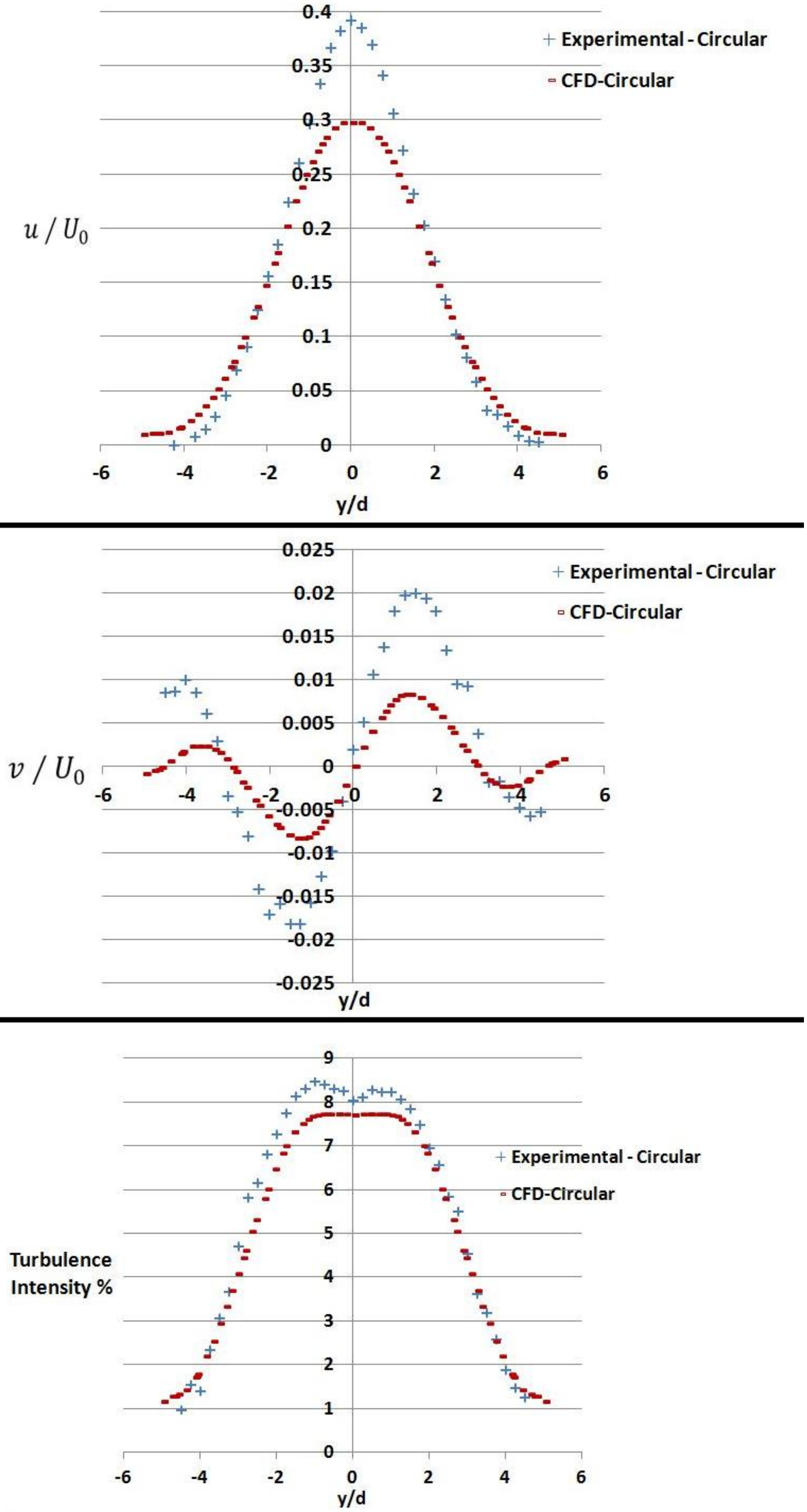

Figure 3.7 : Dimensionless u velocity, v velocity and turbulence intensity in the direction perpendicular to the flow at x/d=20.

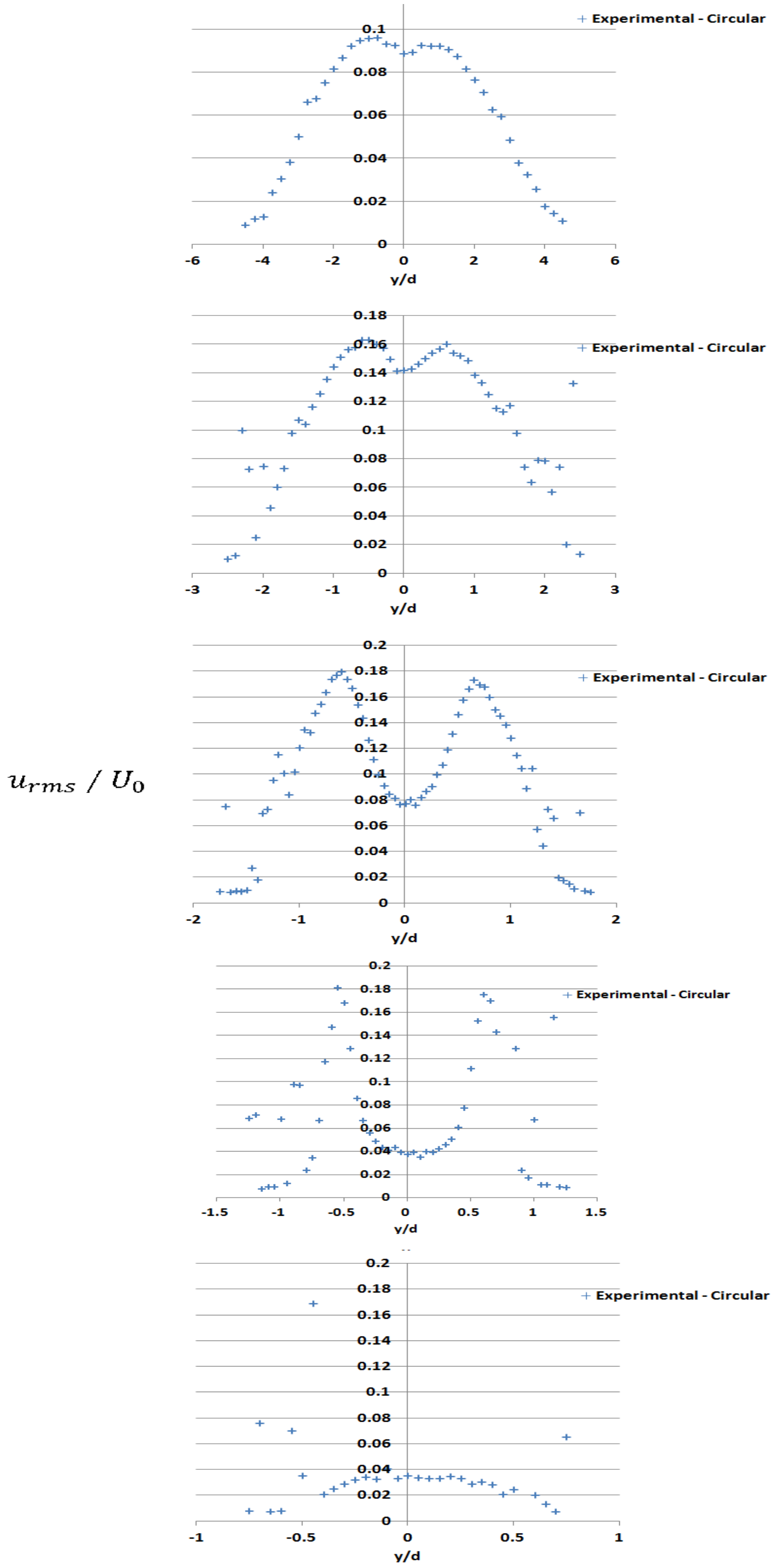

Figure 3.8 : u_{rms} / U_0 distribution (experimental) for circular nozzle at x/d= 20, 10, 5, 2 and 0.3 (from top to bottom).

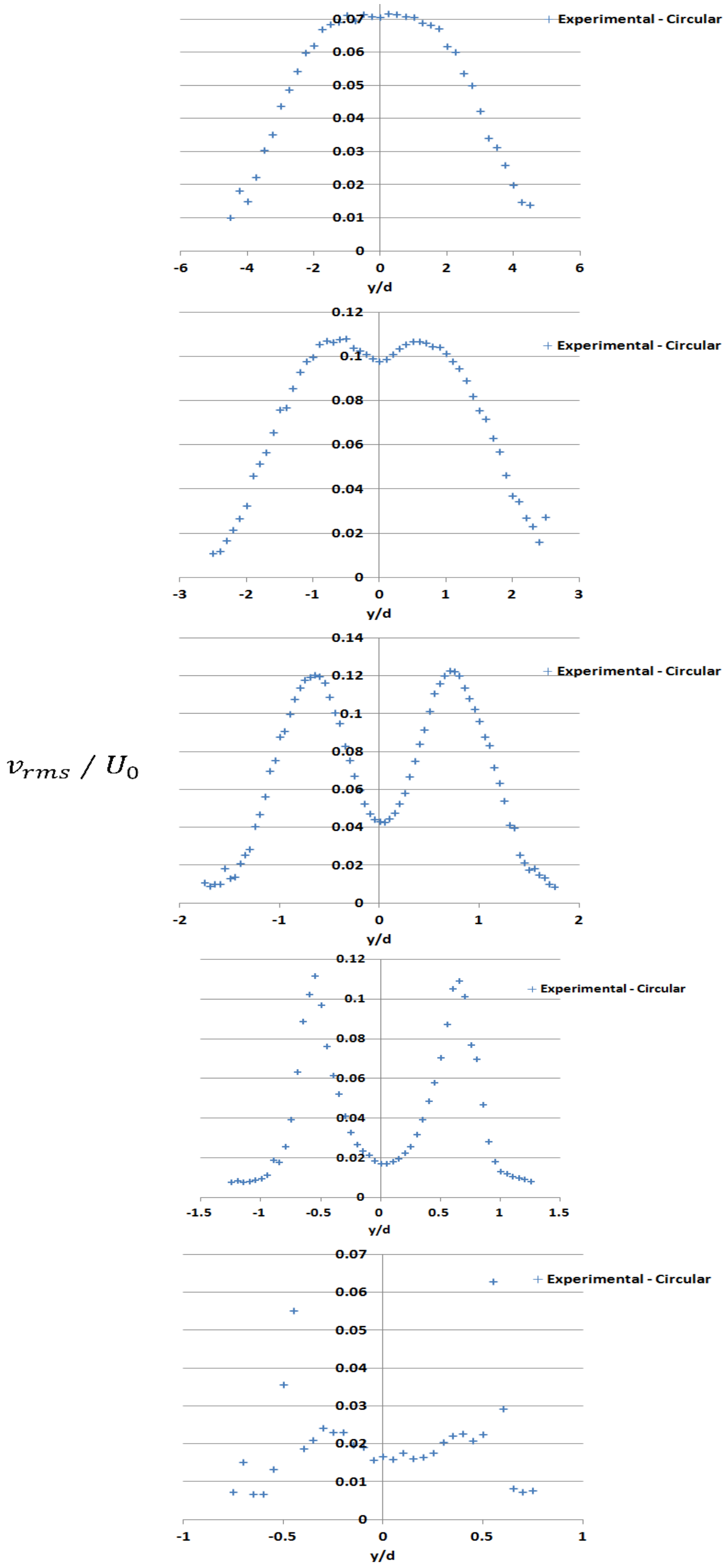

Figure 3.9 : v_{rms} / U_0 distribution (experimental) for circular nozzle at x/d= 20, 10, 5, 2 and 0.3 (from top to bottom)**.**

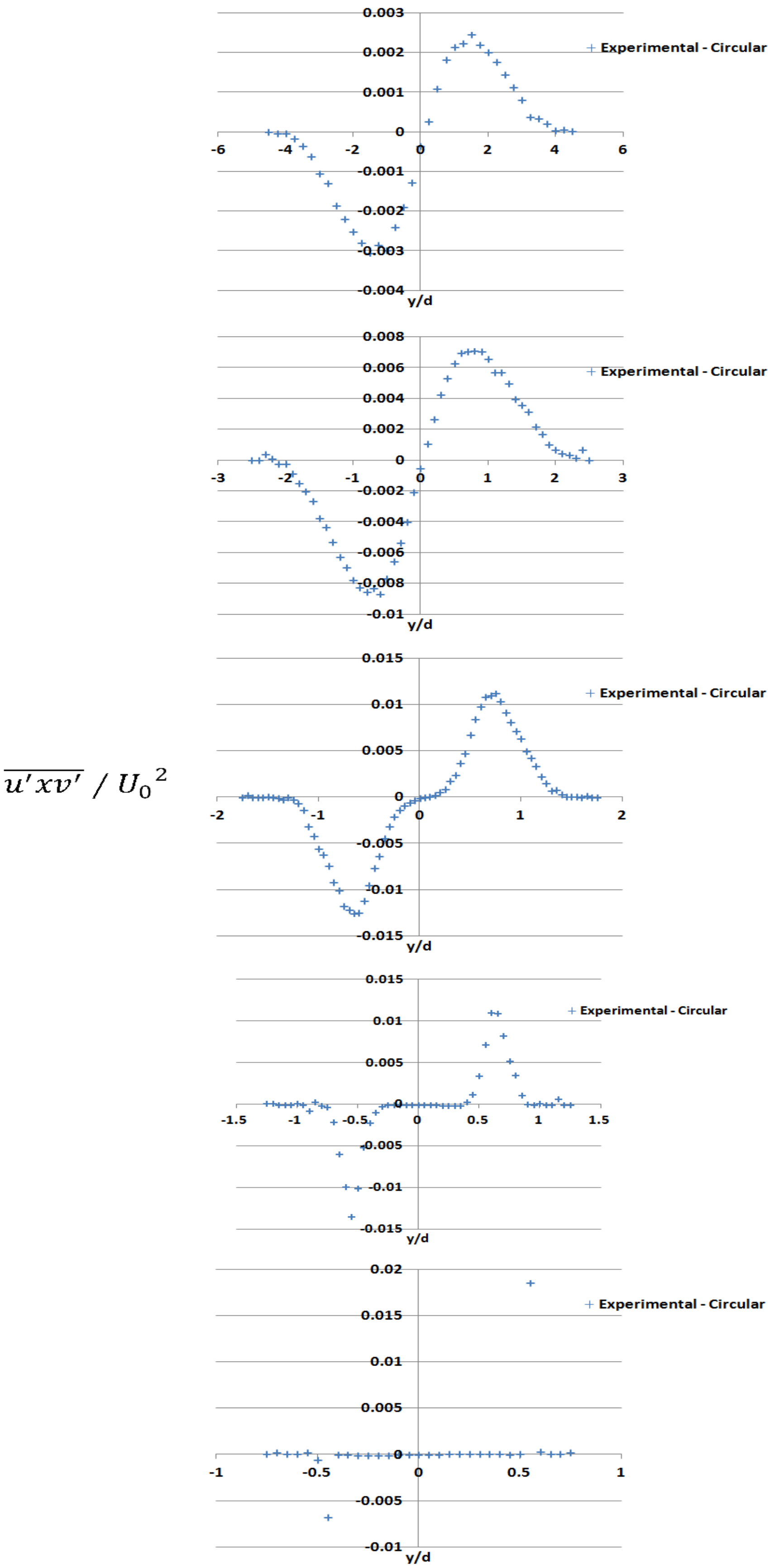

Figure 3.10 : $\overline{u' \times v'}\ /\ U_0{}^2$ distribution (experimental) for circular nozzle at x/d= 20, 10, 5, 2 and 0.3 (from top to bottom).

Following the validation, comparison of three different exit geometries was started. First parameter was u/U_0 distribution and the results are shown in Figure 3.7. While jet flow from the 3 lobed geometry maintains its initial velocity further downstream, its rate of decay is larger in the following section.Rhombus nozzle flow decays faster than both circular and 3 lobed nozzles. But it converges to circular nozzle flow until approximately x/d=25. After x/d=25 rhombus and circular nozzle flow u/U_0 distribution is coincident.

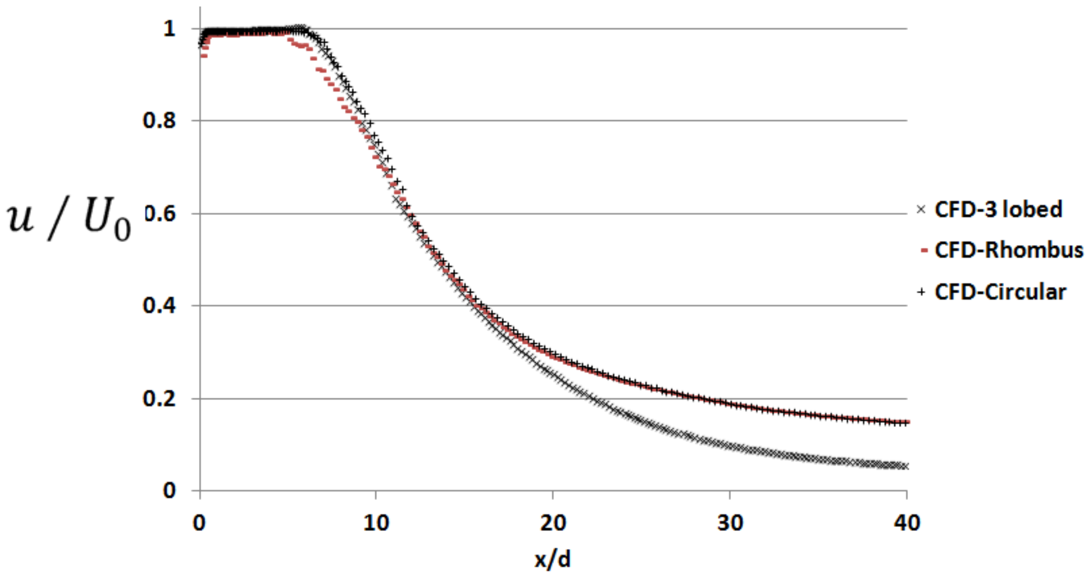

Figure 3.11 : Dimensionless u velocity distribution on the jet centerline for the three different jet flows.

Turbulence intensity distribution is shown in Figure 3.12. Rhombus nozzle flow turbulence intensity starts to increase at x/d=5 while 3 lobed and circular turbulence intensity values stats to increase after x/d=5 with nearly the same rate. Both 3 lobed and rhombus nozzle flows have a similar maximum turbulence intensity value which is smaller than the circular nozzle flow. For 3 lobed flow, turbulence intensity decreases faster after a point between x/d=10 and 15 and results in lower values in the far downstream region when compared with rhombus and circular.

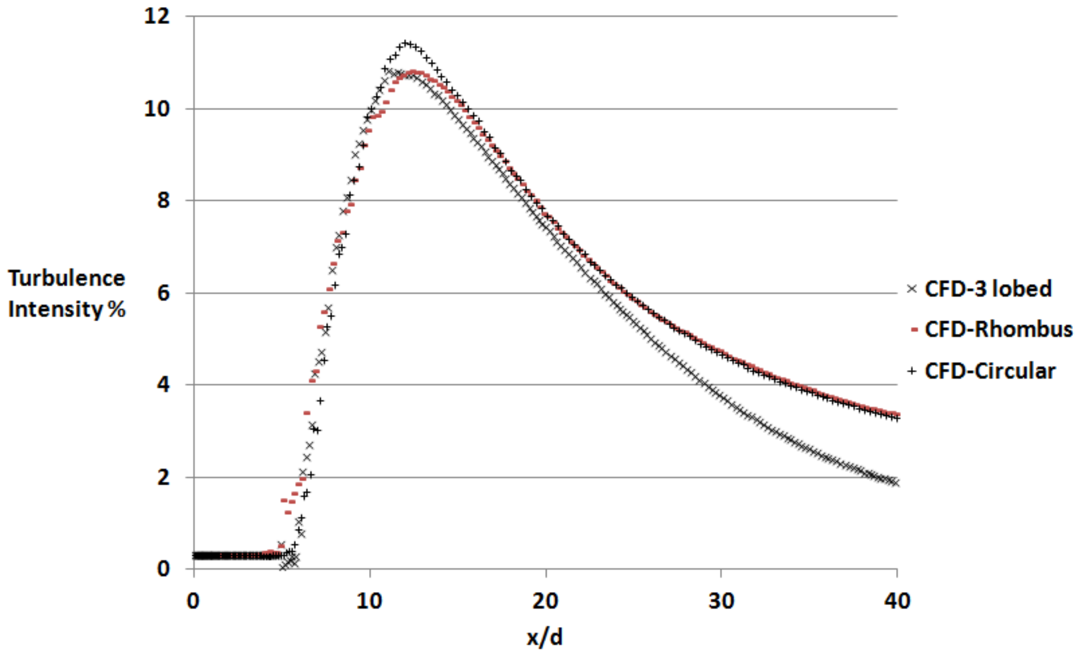

Figure 3.12 : Turbulence intensity distribution on the jet centerline for the three different jet flows.

Following the above mentioned results, characteristic of the flow issuing from rhombus exit was discussed in detail. First dimensionless u velocity distributions at cross-sections at x/d= 2, 5, 7, 10, 15 and 20 were shown in Figure 3.13 and Figure 3.14. Isocurves starts with a rhombus shape all over the cross-section at x/d=2. There is a sharp transition between the high velocity region in the center to the ambient velocity, i.e. u=0, on a narrow region around the nozzle lip. This region gets wider and the transition gets smoother when moved downstream. In addition, transition from rhombus to circular shape takes place starting from the outer region when moved from x/d=2 to x/d=20.

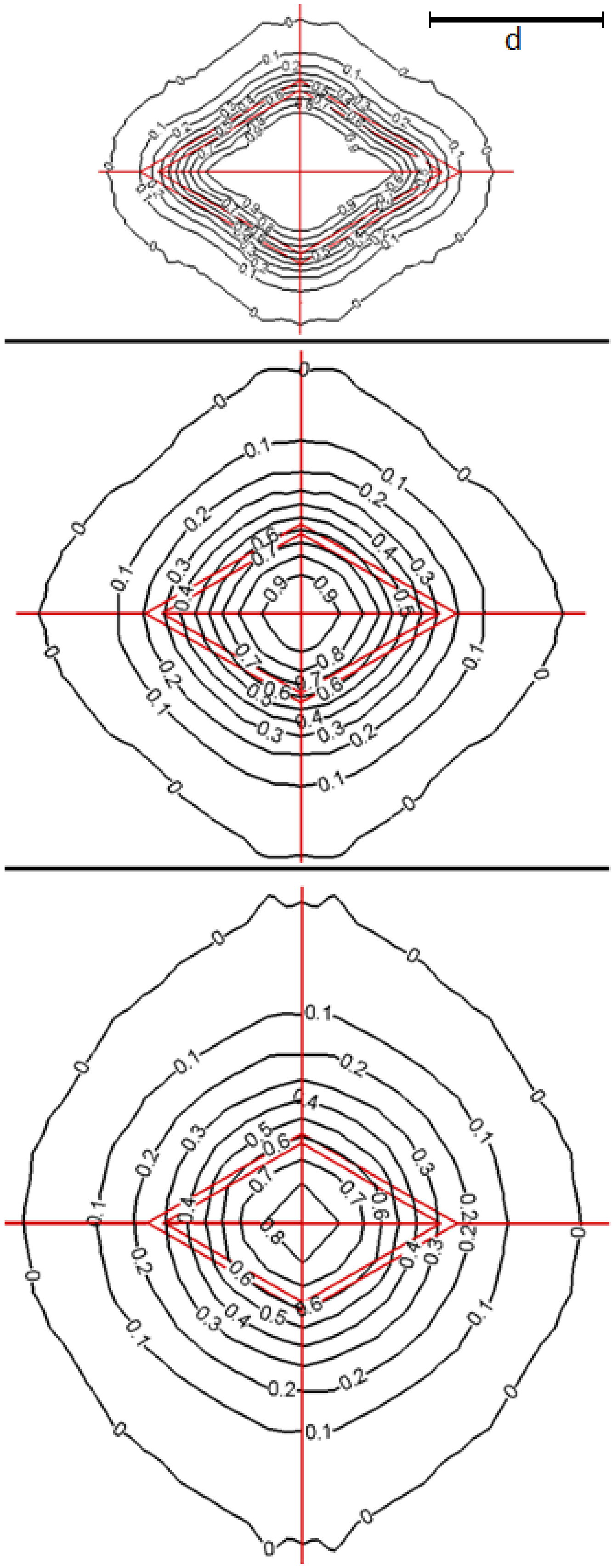

Figure 3.13 : Dimensionless u velocity (u/U_0) distribution at x/d=2, 5 and 7 (from top to bottom).

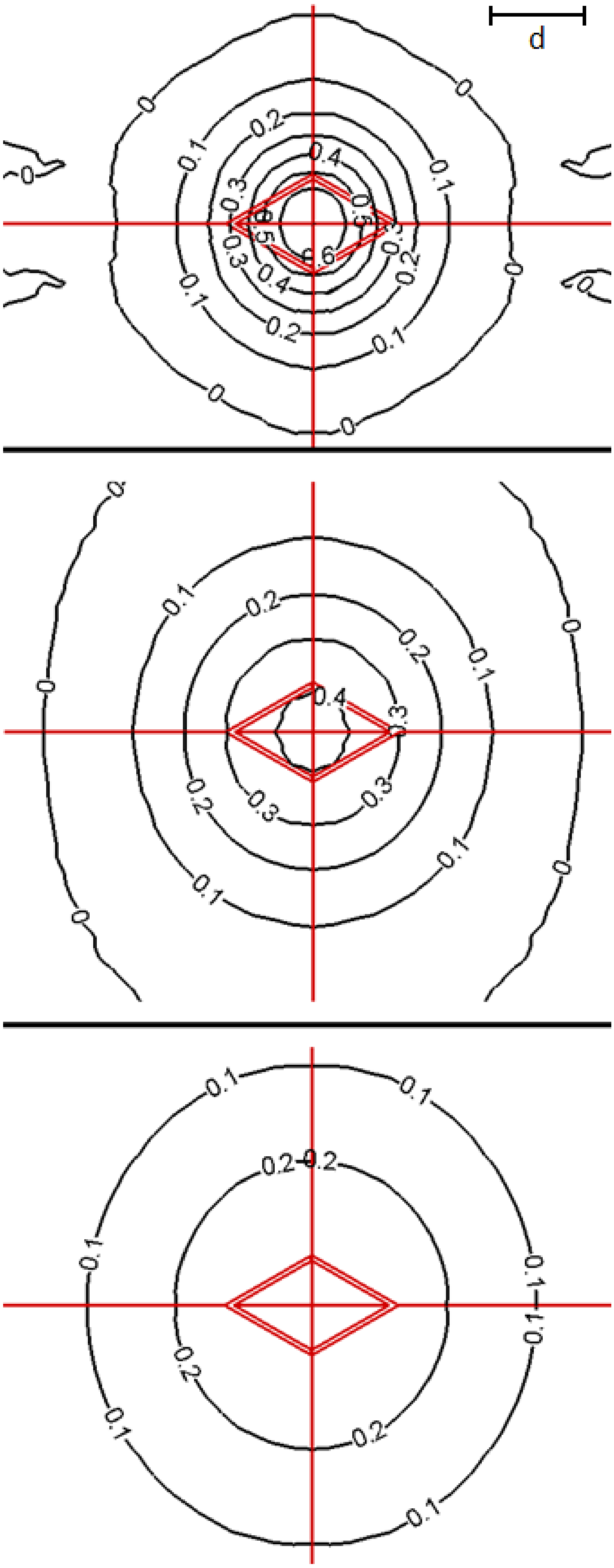

Figure 3.14 : u/U_0 distribution at x/d=10, 15 and 20 (from top to bottom).

Turbulence intensity isocurves at the cross-section at x/d=2 are shown in Figure 3.15. In the center there is a region of low turbulence intensity. Turbulence intensity increases towards the nozzle lip. There is a sharp increase near the lip region where the shear layer is present. In the radial direction, turbulence intensity values decrease again after this region.

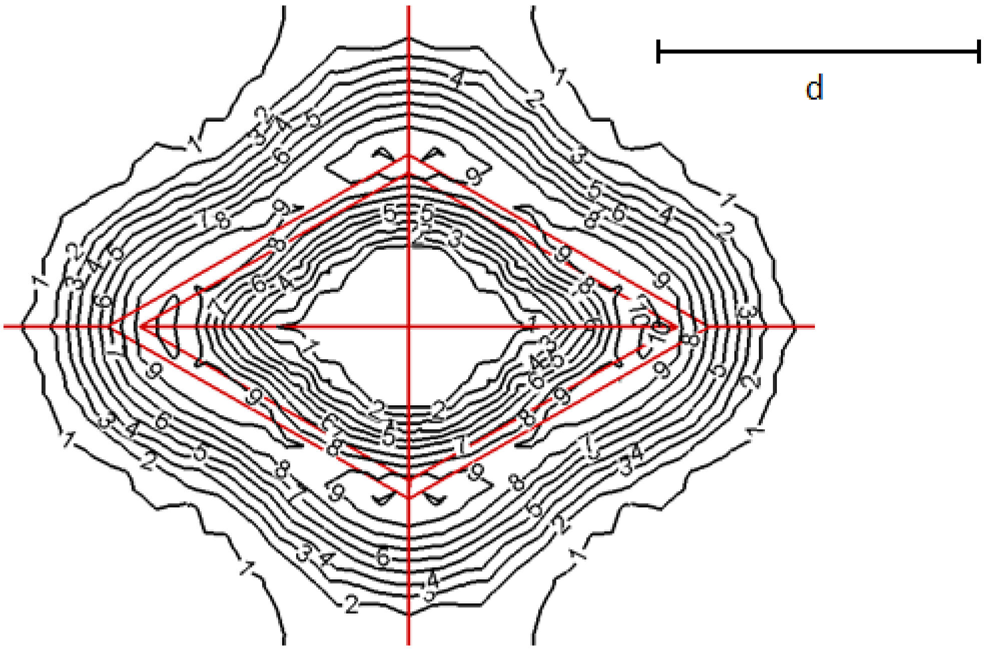

Figure 3.15 : Turbulence intensity distribution at x/d=2.

In the cross-sections at x/d=5 and 7, the same trend holds for turbulence intensity whose distribution is shown in Figure 3.16. But turbulence intensity values in the center increases so there is a smoother transition. Also the cross sectional area of the turbulent flow increases as we move downstream and the isocurves in the outer region takes circular shape.

Additional move downstream results in a circular distribution rather than rhombus. The effect of the lip vanished; maximum value takes place in the center and decreases in the radial direction. Turbulence intensity distribution at x/d=10, 15 and 20 is shown in Figure 3.17.

u velocity distribution at x/d=2, 5 and 7 of 3 lobed flow is shown in Figure 3.18. In this figure the conversion from 3 lobed velocity profiles to circular velocity profiles is shown. Also a 180 degree turn of the exit profile can be seen at x/d=5 and 7.

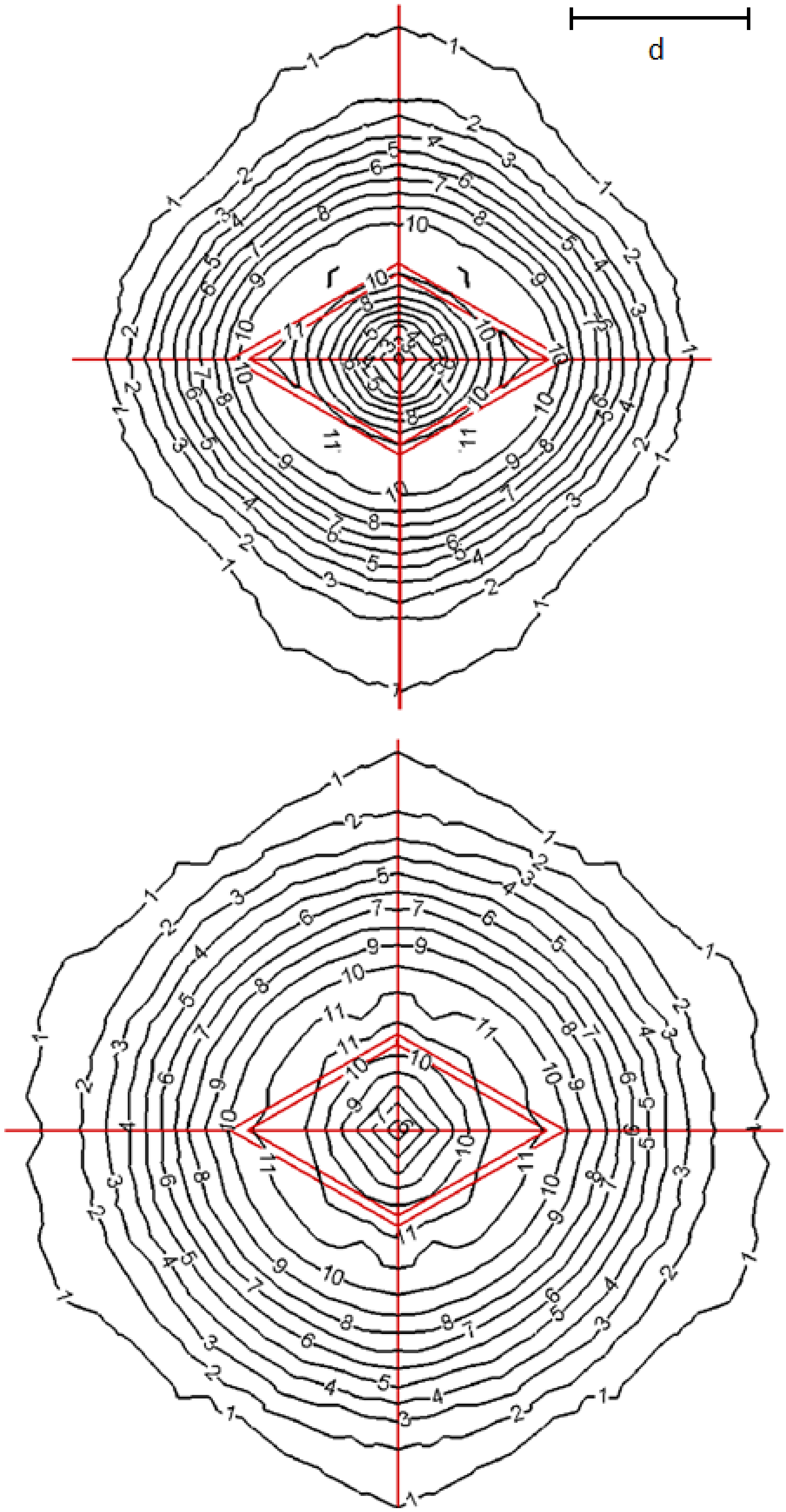

Figure 3.16 : Turbulence intensity distribution at x/d=5 and 7.

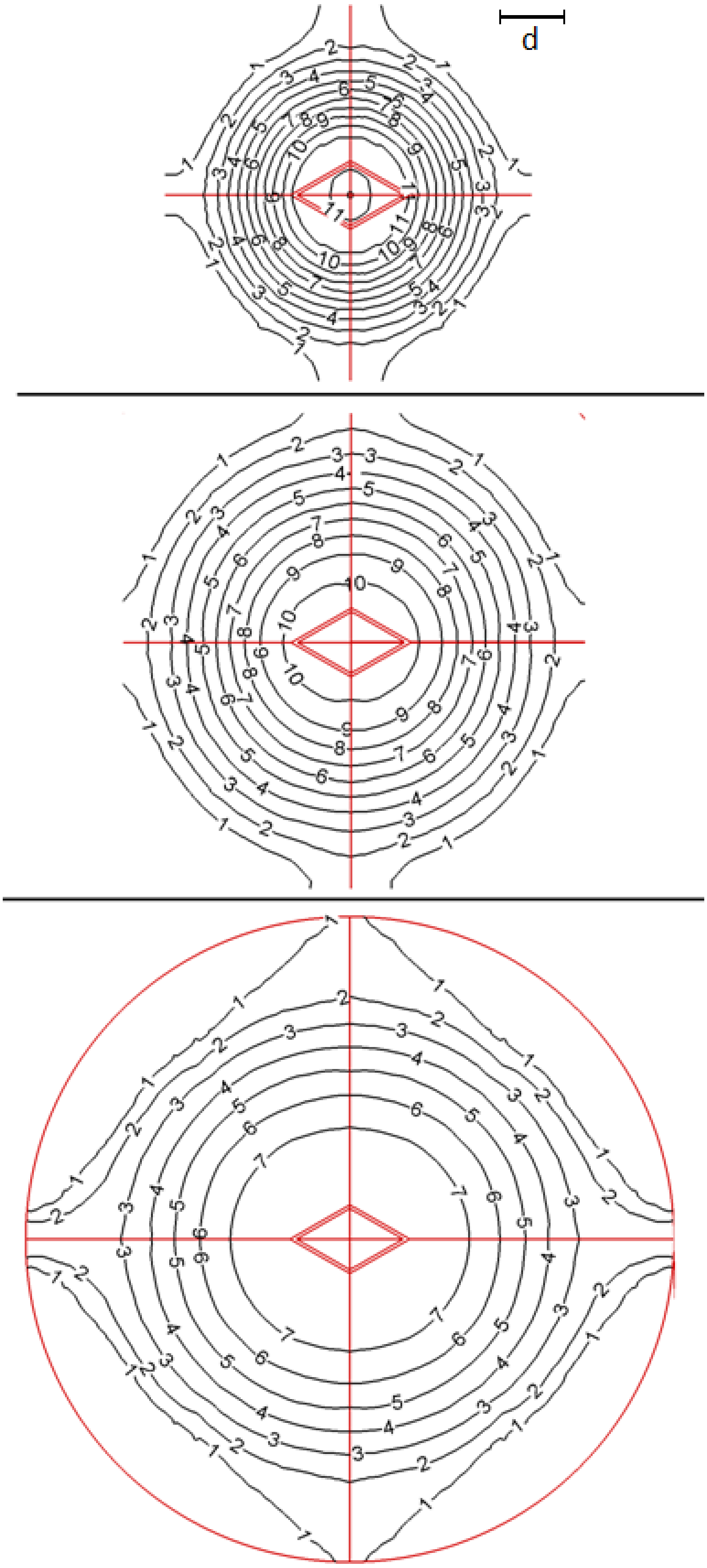

Figure 3.17 : Turbulence intensity [%] distribution at x/d=10, 15 and 20 (from top to bottom).

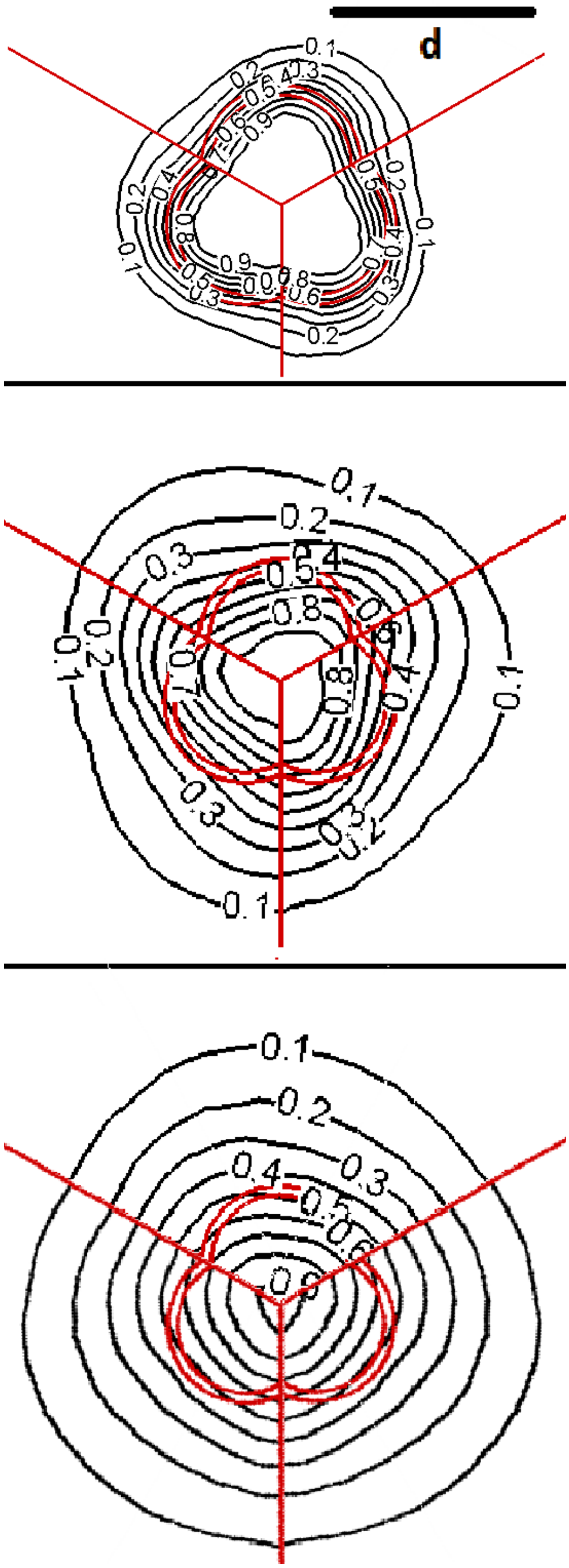

Figure 3.18 : Dimensionless u velocity ($^{u}/_{U_0}$) distribution at x/d= 2, 5 and 7 (from top to bottom).

Distribution of u velocity at x/d=10, 15 and 20 is shown in Figure 3.19. While a triangular shape can still be seen at the center at x/d=10, from this point downstream all velocity profiles are circular.

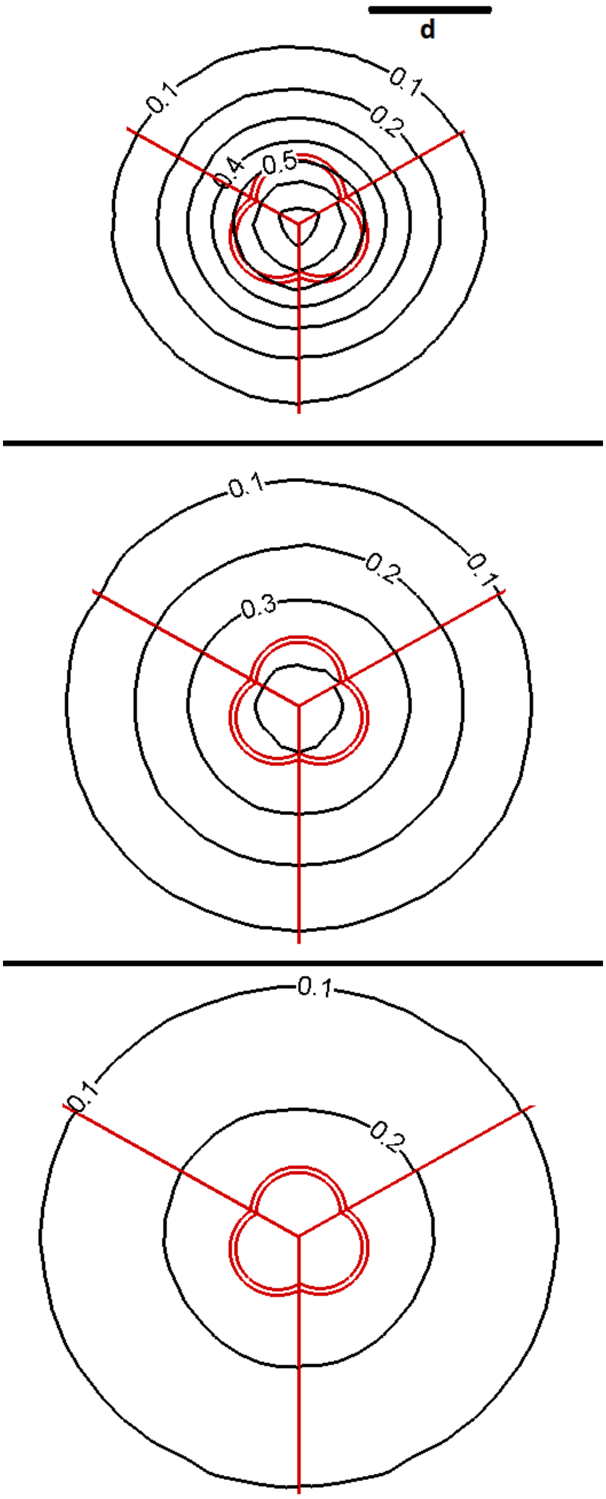

Figure 3.19 : Dimensionless u velocity (u/U_0) distribution at x/d= 10, 15 and 20 (from top to bottom).

Turbulence intensity distribution of the 3 lobed flow at x/d=2, 5 and 7 is shown in Figure 3.20 while turbulence intensity distribution of the 3 lobed flow at x/d=10, 15 and 20 is shown in Figure 3.21. In these figures the 180 of the exit flow profile can be more explicitly seen at x/d=2 and 5. This axis switching is an important property of such flows. This phenomena caused some kind of swirl in the 3 lobed flow as a difference from rhombus flow thus increased the turbulence intensity around the main flow.

Jet half width, $y_{0.5}$, which is the radial location where the jet u velocity is half the value at the jet centerline at a specified yz plane is plotted for 3 lobed and rhombus flows and shown in Figure 3.22. In this figure it is shown that the profiles far downstream takes a circular shape and profiles converge to each other for the two different geometries. The 180 degree turn of the 3 lobed flow profile can be seen at x/d=5.

.

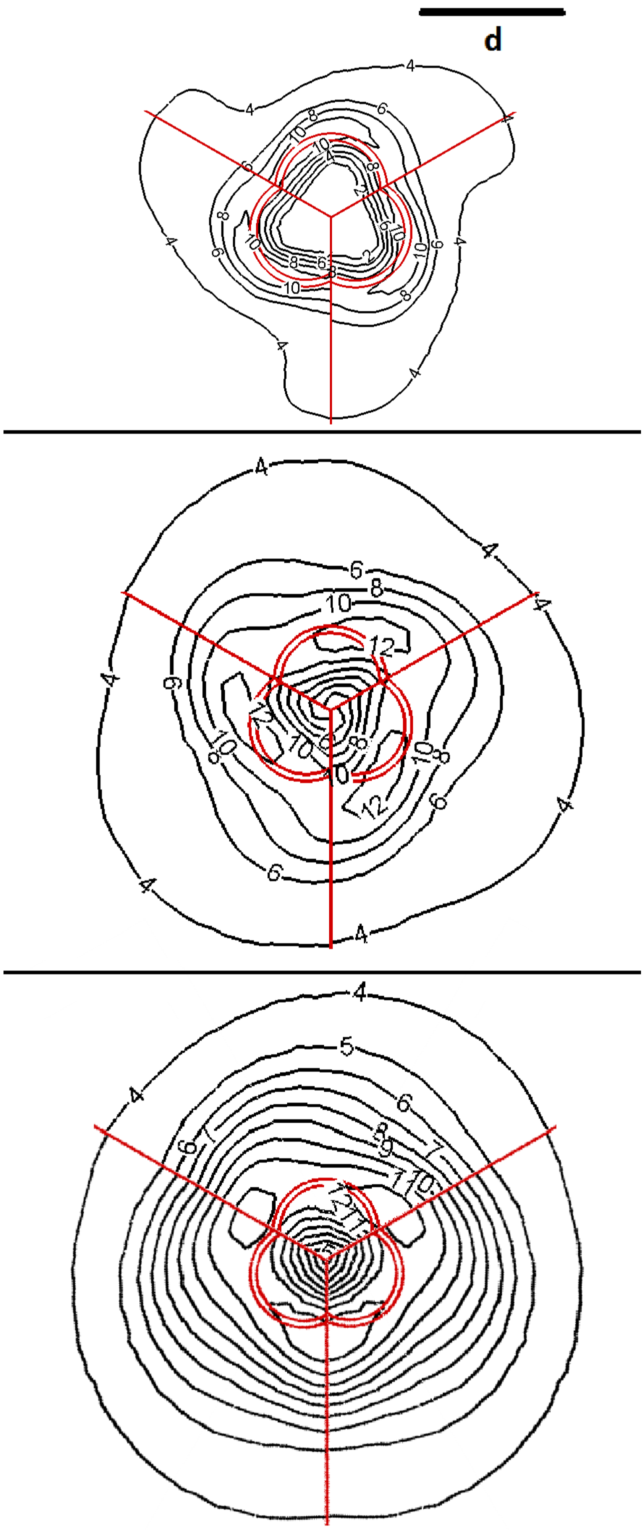

Figure 3.20 : Turbulence intensity [%] distribution of 3 lobed flow at x/d=2, 5 and 7 (from top to bottom).

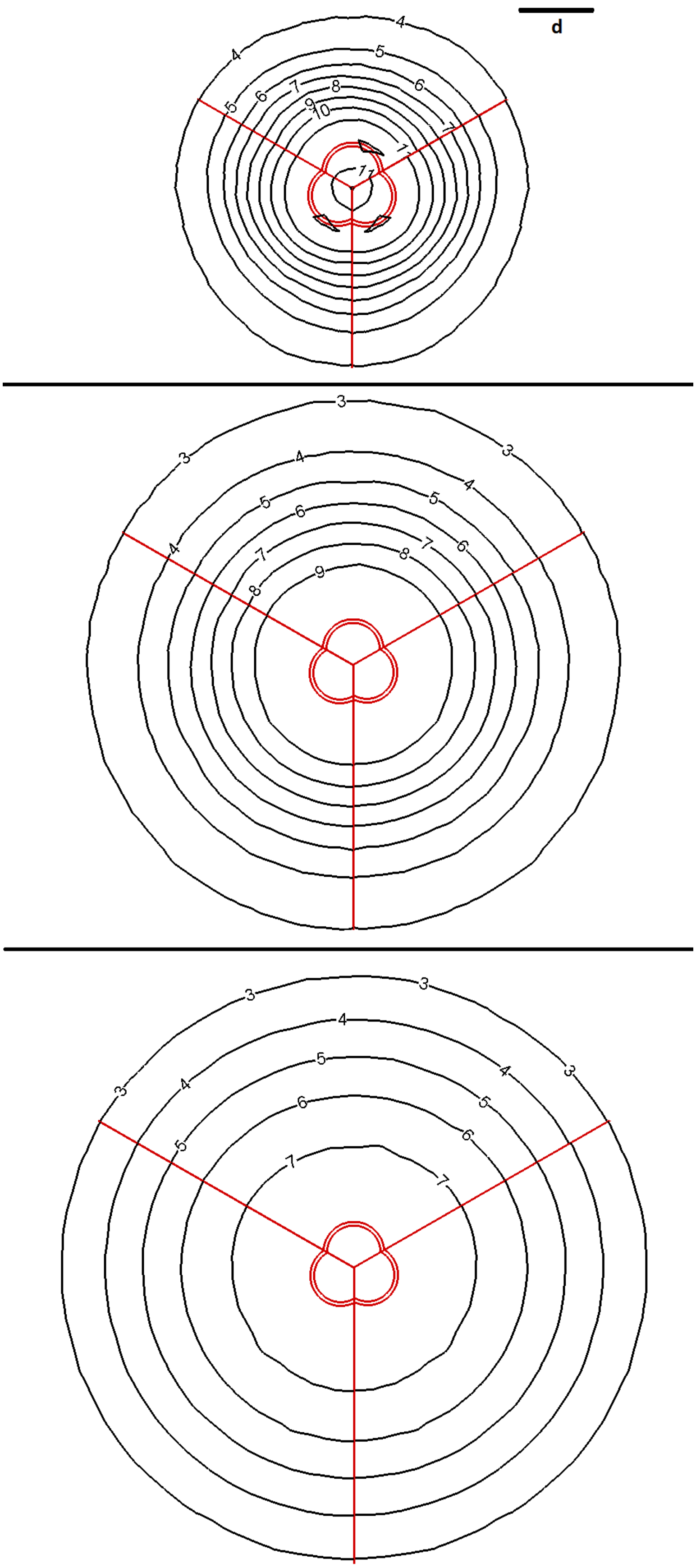

Figure 3.21 : Turbulence intensity [%] distribution of 3 lobed flow at x/d=10, 15 and 20 (from top to bottom).

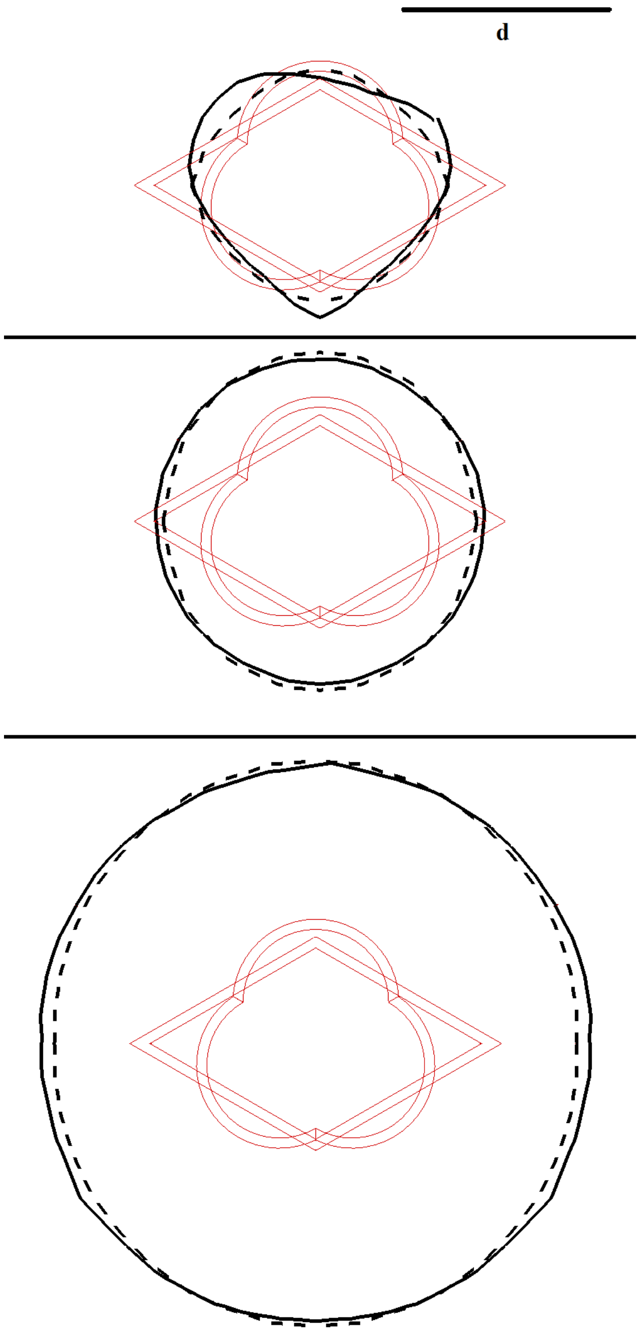

Figure 3.22 : $y_{0.5}$ curves at x/d=5, 10 and 15 for 3 lobed and rhombus flows.

4. CONCLUSION

Jet flow is an important flow type which has a wide range of application in engineering. Understanding the characteristics of jet flow in conjunction with the nozzle which the jet issues from is critical to control these characteristics. In this study effect of different nozzle exit geometries on the characteristics of jet flew was studied. CFD results were validated against experimental results. k-ε turbulence model which is a RANS model was interpreted to be a good choice as it delivers results with a sufficient accuracy. Laser Doppler Anemometry was used to measure velocity distribution in the flow thus the turbulence. Characteristics of flows issuing from nozzles with different exit geometries were compared and performance was interpreted. In the future tendency of flow characteristic changes due to the changes in these nozzle shapes might be a subject to be studied. Also, noise inducing flow structures might be investigated and effect of the nozzle shapes can be studied in detail.

REFERENCES

ANSYS, Inc (2009) Fluent Theory Guide, ANSYS, Inc

ANSYS, Inc (2006) Fluent 6.3 User's Guide, ANSYS, Inc

Garcia. R. G. (2007) CFD simulation of flow fields associated with high speed jet impingement on deflectors, MSc Thesis, Virginia Polytechnic University and State University

Gohil, T. B., Saha, A.K., Muralidhar K.(2014) Large Eddy Simulation of a Free Circular Jet, Journal of Fluids Engineering, ASME MAY 2014, Vol. 136.

Gutmark, E. J., Grinstein, F. F. (1999) Flow Control with Noncircular Jets, Annu. Rev. Fluid Mech., Vol. 31, p.239–272, 1999

Hilgers, A., Control and optimization of turbulent jet mixing, Center for Turbulence Research Annual Research Briefs, 2000, pp45-54

Hu, H., Saga, T., Kobayashi, T., Taniguchi, N. (2002) Mixing Process in a Lobed Jet Flow, AIAA Journal, Vol. 40, p: 1339-1345

Schadow, K. C., Gutmark, E. J., Parr, D. M., Wilson, K. C. (1988) Selective control of flow coherence in triangular jets, Exp. Fluids, Vol. 6, p: 129-135

Toyoda K. and Hussein A.K.M.F. (1989) Vortical Structures of Noncircular Jets, Proceedings of 4th Asian Congress of Fluid Mechanics, p:A117-127, 1989

Vandsburger U. and Ding C. (1995) The spatial modulation of a forced triangular jet, Exp. Fluids, Vol. 18, p: 239-248

Yukselenturk, Y. and Erdem, D. (2012) An experimental study on the near flow field characteristics of noncircular jets, International Conference Experimental Fluid Mechanics, Hradec Kralove, Czech Republic, 20-23 November 2012.

Zaman K. B. M. Q., Wang F. Y., Georgiadis N. J.(2002) Noise, Turbulence and Thrust of Subsonic Freejets from Lobed Nozzles, AIAA Journal, Vol. 41, p:398-407, March 2003

CURRICULUM VITAE

Name Surname: **Yavuzer Karakuş**

Place and Date of Birth: **19/07/1986**

E-Mail: **karakusy@itu.edu.tr**

EDUCATION

B.Sc.: Aeronautical Engineering, Istanbul Technical University

PROFESSIONAL EXPERIENCE AND REWARDS

Aerodynamics Engineer, TUSAS Engine Industries,
April 2012 – November 2013

Research Assistant, Istanbul Technical University Aeronautical Engineering Department
December 2013- Present

PUBLICATIONS, PRESENTATIONS AND PATENTS ON THE THESIS:

- Effect of Nozzle Exit Geometry on Jet Flow, Seminar Presentation at Istanbul Technical University Faculty of Aeronautics and Astronautics as a part of the Master Program Curriculum

OTHER PUBLICATIONS, PRESENTATIONS AND PATENTS :

- Karakus, Y., Kavas, I., Yasa, T., 2014: Aero-thermal Investigation of Turbulator Cross Section Shape on Turbine Blade Cooling, International Symposium on Convective Heat and Mass Transfer, June 8-13, 2014 Aydın, Turkey.
- Inanli, S., Yasa, T., Karakus, Y., Kavas, I., 2013: An Internal Cooling Test Bench for Gas Turbine Research, 7th Ankara International Aerospace Conference, September, 2013, Ankara/Turkey.